

## In-Depth Analysis of Chiroptical Properties of Enones Derived from Abietic Acid

Marek Masnyk, Aleksandra Butkiewicz, Marcin Górecki, Roman Luboradzki, Piotr Paluch, Marek J. Potrzebowski, and Jadwiga Frelek

*J. Org. Chem.*, **Just Accepted Manuscript** • DOI: 10.1021/acs.joc.7b02911 • Publication Date (Web): 01 Mar 2018

Downloaded from <http://pubs.acs.org> on March 2, 2018

### Just Accepted

“Just Accepted” manuscripts have been peer-reviewed and accepted for publication. They are posted online prior to technical editing, formatting for publication and author proofing. The American Chemical Society provides “Just Accepted” as a service to the research community to expedite the dissemination of scientific material as soon as possible after acceptance. “Just Accepted” manuscripts appear in full in PDF format accompanied by an HTML abstract. “Just Accepted” manuscripts have been fully peer reviewed, but should not be considered the official version of record. They are citable by the Digital Object Identifier (DOI®). “Just Accepted” is an optional service offered to authors. Therefore, the “Just Accepted” Web site may not include all articles that will be published in the journal. After a manuscript is technically edited and formatted, it will be removed from the “Just Accepted” Web site and published as an ASAP article. Note that technical editing may introduce minor changes to the manuscript text and/or graphics which could affect content, and all legal disclaimers and ethical guidelines that apply to the journal pertain. ACS cannot be held responsible for errors or consequences arising from the use of information contained in these “Just Accepted” manuscripts.



# In-Depth Analysis of Chiroptical Properties of Enones Derived from Abietic Acid

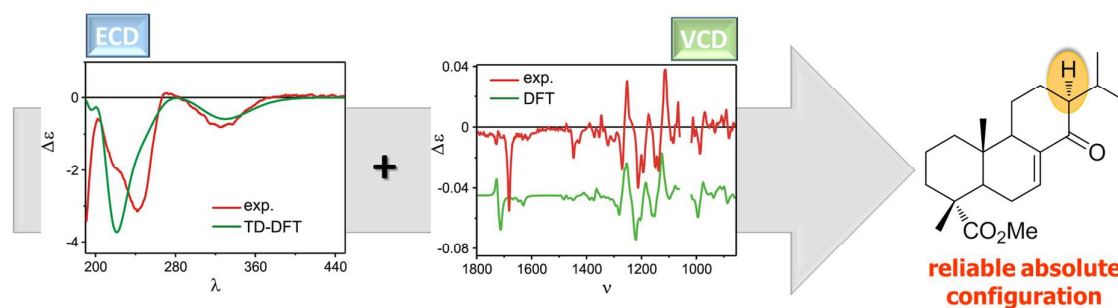
Marek Masnyk,<sup>\*†</sup> Aleksandra Butkiewicz,<sup>†</sup> Marcin Górecki,<sup>†</sup> Roman Luboradzki,<sup>‡</sup> Piotr Paluch,<sup>§</sup> Marek J. Potrzebowski,<sup>§</sup> and Jadwiga Frelek,<sup>\*†</sup>

<sup>†</sup> *Institute of Organic Chemistry, Polish Academy of Sciences, Kasprzaka 44/52, 01-224 Warsaw, Poland;*

<sup>‡</sup> *Institute of Physical Chemistry, Polish Academy of Sciences, Kasprzaka 44/52, 01-224 Warsaw, Poland;*

<sup>§</sup> *Centre of Molecular and Macromolecular Studies, Polish Academy of Sciences, Sienkiewicza 112, 90-363 Lodz, Poland*

[marek.masnyk@icho.edu.pl](mailto:marek.masnyk@icho.edu.pl); [jadwiga.frelek@icho.edu.pl](mailto:jadwiga.frelek@icho.edu.pl);



## Abstract

With the use of inexpensive commercially available abietic acid, a whole series of abietane enones have been prepared in high yields. The structures of all the products obtained were determined by comprehensive spectroscopic analysis with particular emphasis on the use of advanced NMR techniques, comparison with previously reported data, and where possible by single crystal X-ray diffraction. However, in cases where X-ray crystallography was not applicable or compounds tested were unstable, a final stereochemical assignment could be only inferred by electronic circular dichroism (ECD) supported by vibrational circular dichroism (VCD) to increase credibility. To reveal the relationship between structure and chiroptical properties we used combined experimental and theoretical analysis of geometries,

1  
2  
3 structural parameters and chiroptical properties of all enones synthesized. A thorough analysis  
4 of their conformational flexibility by examining the effect of solvent and temperature on the  
5 ECD spectra was also used to achieve desired objectives. As a result, the impact of  
6 substituents adjacent to the enone chromophore on the conformation was determined by  
7 demonstrating that even slight changes in the position of hydroxyl and isopropyl groups  
8 attached to carbon C13 may substantially affect ECD curves' pattern leading in some cases to  
9 Cotton effects' sign reversal.  
10  
11  
12  
13  
14  
15  
16  
17

## 18 INTRODUCTION

19  
20 It is widely recognized that biological activity of molecules is highly driven by their three-  
21 dimensional structure. An example of this is the strong dependence of physiological or  
22 pharmacological properties on the chiral recognition by chiral receptors, interacting  
23 predominantly with molecules or phases of the correct spatial arrangement.<sup>1</sup> Therefore, access  
24 to methods appropriate for the reliable absolute configuration (AC) assignment and detailed  
25 structural analysis is of paramount importance. Here, chiroptical methods, including in  
26 particular circular dichroism (CD), not only meet but also successfully fulfil such a  
27 requirement. The recent progress in *ab initio* methods and computer sciences additionally  
28 makes the application of quantum chemical calculations of molecular and chiroptical  
29 properties enforceable.<sup>2</sup> Consequently, the reliability of the assignment of the AC, as a result  
30 of combined experimental-theoretical analysis of the CD results, is unquestionably multiplied,  
31 thus leading to their increasingly frequent and efficient use.<sup>3</sup> Nevertheless, examples can be  
32 found that lead to ambiguous results even when using many different chiroptical techniques  
33 combined with quantum-chemical calculations. One such exemplary group of compounds are  
34  $\alpha,\beta$ -enones that have been investigated extensively over the past decades, both experimentally  
35 and theoretically, in terms of electronic circular dichroism (ECD) spectroscopy.<sup>4</sup> The interest  
36 in enones was undoubtedly related to the fact that this chromophore is one of the most popular  
37  
38  
39  
40  
41  
42  
43  
44  
45  
46  
47  
48  
49  
50  
51  
52  
53  
54  
55  
56  
57  
58  
59  
60

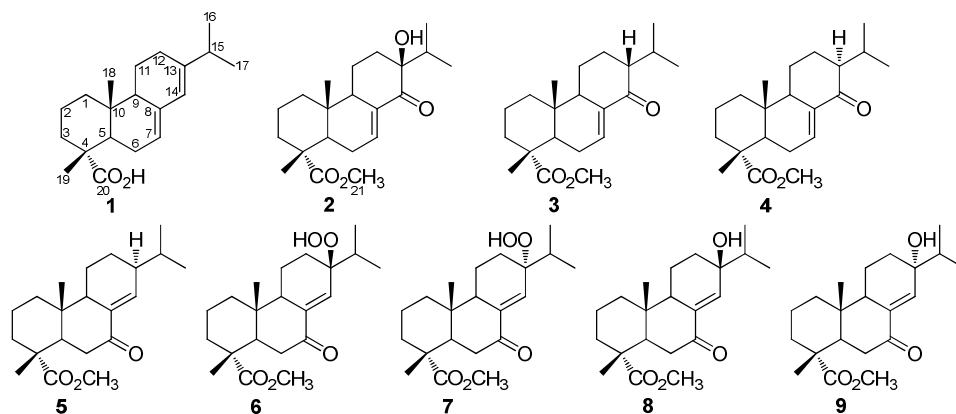
1  
2  
3 structural motifs found in numerous natural products exhibiting, in most cases, essential  
4 biological activity. Steroids, terpenoids, and alkaloids can be listed as examples of such  
5 biologically relevant compounds with enone units in their skeletons.<sup>5</sup> Also, their defined  
6 absorption in the UV-Vis region together with a stiffening of the molecular skeleton, thus  
7 reducing the number of conformers contributing to the ECD spectra, resulted in their selection  
8 as suitable model systems for chiroptical studies. As a result of intensive chiroptical  
9 investigations, a number of sector and helicity rules correlating signs and magnitudes of  
10 observed Cotton effects (CEs) in the ECD spectra with three-dimensional structure of  $\alpha,\beta$ -  
11 enone molecules have been developed over the years.<sup>4c</sup> In most cases, the torsional angle of  
12 the enone chromophore  $C_\beta=C_\alpha-C=O$ , defined as  $\omega$ , determines the sign of the CE associated  
13 with the  $n-\pi^*$  transition occurring at around 320-350 nm.<sup>4a, 4c</sup> A satisfactory correlation  
14 between ECD and stereochemistry might also be found for the  $\pi-\pi^*$  type transitions of  $\alpha,\beta$ -  
15 enones.

16  
17  
18  
19  
20  
21  
22  
23  
24  
25  
26  
27  
28  
29  
30  
31 Gawroński, however, showed the significant effect of the enone dissymmetry and  
32 substituents present in the proximity of the chromophore on the shape of the spectra in this  
33 spectral region.<sup>4a, 4c</sup> His finding leads to the conclusion that the above factors may have a  
34 dramatic impact on the UV and ECD spectra of  $\alpha,\beta$ -unsaturated ketones forcing, in some  
35 cases, the reformulation or even change of the working rules.<sup>3d</sup> As demonstrated in numerous  
36 works exploring the three-dimensionality of enones *via* chiroptical properties remains a  
37 nontrivial task and may become a complicated issue in cyclic  $\alpha,\beta$ -enones.<sup>3d, 4d, 6</sup> We have been  
38 additionally motivated to continue research in this area, by our latest results demonstrating  
39 that in some cases the sign of the  $n-\pi^*$  ECD signals in enones could not be satisfactorily  
40 described by a minimum structure model.<sup>3d</sup> Therefore, further detailed studies on this topic  
41 are justified, if not necessary, as they can lead to the clarification of ambiguities and doubts  
42 still present in the field. These studies should further aid the thorough exploration of the  
43  
44  
45  
46  
47  
48  
49  
50  
51  
52  
53  
54  
55  
56  
57  
58  
59  
60

1  
2  
3 structure-property relationships and find out how even subtle structural changes modulate  
4  
5 them. This work is undertaken exactly for this purpose, assuming that the *cis*-enone  
6  
7 chromophore in the selected new structures should contain substituents in its environment to  
8  
9 allow a methodical comparative analysis. With new model compounds in hand, their  
10  
11 chiroptical properties will be carefully analyzed for compliance with the above-specified  
12  
13 objectives. The resulting access to more experimental data should enable clarification of the  
14  
15 existing controversies or at least reduce their numbers. It could also play a significant role in  
16  
17 creating and/or developing new theories. In doubtful cases, which cannot be excluded,  
18  
19 vibrational circular dichroism (VCD) will be used to support and verify the ECD results and  
20  
21 thus achieve strengthening of the conclusions drawn. As VCD is the extension of the  
22  
23 electronic CD into infrared/near-infrared absorption region of the spectrum, *i.e.*, where  
24  
25 vibrational transitions occur within the ground electronic state of the molecule, therefore it  
26  
27 provides new information about structural features of chiral molecules. Consequently, an  
28  
29 approach based on two independent dichroic methods leads to the reinforcement of  
30  
31 stereochemical argumentation.  
32  
33

34  
35 When looking for model compounds, our attention turned to abietane diterpenes. The  
36  
37 abietane-type diterpenoids often exhibit outstanding biological activity which is why they  
38  
39 were and are used in therapy, including folk medicine.<sup>7,8</sup> Their unique architecture and  
40  
41 structural diversity, places them as a good starting point for the synthesis of a variety of *cis*-  
42  
43 enones. As a substrate for the planned synthesis, we have chosen abietic acid **1** (Chart 1): a  
44  
45 natural product which is a major component of resin acids abundantly occurring in conifer  
46  
47 oleoresin, used commercially in paints, varnishes, and lacquers. The benefit of using abietic  
48  
49 acid as a substrate in synthesis is its low price. What is more, it was also effectively used for  
50  
51 the synthesis of a wide variety of complex molecules, including other terpenes.<sup>9</sup> The review  
52  
53 of relevant literature has demonstrated the ability to obtain appropriate *cis*-enones through a  
54  
55  
56  
57  
58  
59  
60

1  
2  
3 simple synthesis consisting of a few steps at most.<sup>10</sup> Therefore, taking into account both the  
4 economic as well as the synthetic point of view, we recognized abietic acid as a convenient  
5 starting material for the preparation of a whole range of compounds with suitable  
6 conformationally diverse molecular structures. The prepared and analyzed enones are  
7 presented in Chart 1.  
8  
9  
10  
11  
12



13  
14  
15  
16  
17  
18  
19  
20  
21  
22  
23  
24  
25  
26 **Chart 1.** Enones under consideration.

27  
28  
29 This article is organized as follows: first, we describe the synthesis of individual enones  
30 and their structure determination based on the comprehensive spectroscopic analysis. Then,  
31 we analyze CD spectra of the enones with the aim to clarify the impact of structural changes,  
32 solvent applied, and measurement temperature on dichroic properties. Finally, we summarize  
33 the results and findings achieved.  
34  
35  
36  
37  
38  
39

## 40 41 **RESULTS AND DISCUSSION**

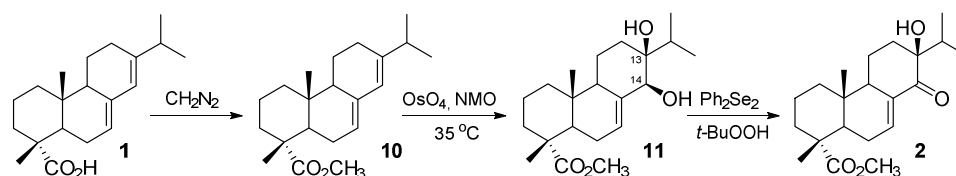
### 42 43 **Synthesis of model compounds**

44  
45  
46 Syntheses of all enones discussed herein were accomplished using commercial abietic acid  
47 **1** (Scheme 1) freshly purified by crystallization of its isoamylamine salt. The synthetic  
48 strategy for preparation of cisoid enones was based on the observations, reported in the  
49 literature, that the particular double bonds within a conjugated diene system in the abietic acid  
50 are susceptible to selective oxidations in which the second double bond remains unchanged.<sup>11</sup>  
51  
52  
53  
54  
55  
56  
57  
58  
59  
60

For our purposes, we adopted *cis*-hydroxylation of the C13-C14 double bond which enabled preparation of 7-en-14-one systems<sup>9b</sup> and iodine-water oxidation suitable for preparation of 8(14)-en-7-one derivatives.<sup>11b</sup>

The first target enone **2** containing 7-en-14-one fragment was prepared by slightly modifying procedure known from literature (Scheme 1).<sup>9b</sup> Abietic acid **1** was esterified with diazomethane and the methyl ester **10** was subjected to selective *cis* hydroxylation with a catalytic amount of osmium tetroxide and *N*-methylmorpholine *N*-oxide as the oxidant in *t*-butyl alcohol/water solution. The resulted diol **11** was then oxidized to hydroxyenone **2** in mild conditions with benzeneselenic anhydride prepared *in situ* from diphenyl diselenide and *tert*-butyl hydroperoxide.

**Scheme 1. Synthesis of enone 2.**

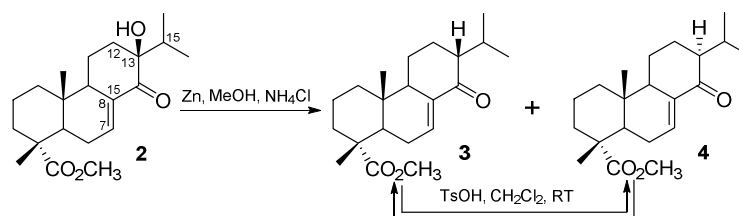


The 13*S*,14*S* absolute configuration of diol **11**, and thus the approach of osmium tetroxide from the  $\beta$ -side in the *cis*-hydroxylation reaction, was confirmed by comparing the literature data of the specific rotation and VCD results.<sup>11a, 12</sup> Similarly, the 13*S* stereochemistry in previously described hydroxyenone **2** has been corroborated by comparing our and literature spectroscopic data.<sup>11a</sup>

Through the preparation of enone **2**, we gained easy access to the next two enones **3** and **4**. Simple reduction of the hydroxyl group in **2** with zinc dust in acidic medium afforded expected epimeric enones **3** and **4** (Scheme 2). The best result, 65% overall yield, was obtained when hydroxyenone **2** was heated at  $50\text{ }^\circ\text{C}$  for a prolonged time in a methanolic solution of ammonium chloride. Reaction yields of the reductions with zinc carried out in boiling methanolic solution of ammonium chloride, boiling methanolic solution of acetic acid

1  
2  
3 or in acetic acid alone at 50 °C were not satisfactory. It is noteworthy that enone **4** with an  
4 axial isopropyl group is vulnerable to acidic isomerization and in the presence of traces of  
5 acid readily converts into isomer **3** with an equatorial isopropyl group. We observed a  
6 significant conversion degree of **4** into **3** afterwards, when the NMR sample of **4** was left in a  
7 deuterated chloroform solution for a couple of hours. In additional experiments under  
8 controlled conditions, **3** and **4** were treated separately with *p*-toluenesulfonyl acid in  
9 dichloromethane solutions at room temperature for 26 hrs. In both reactions the same  
10 mixtures containing 78% of **3** and 22% of **4** were obtained.

### Scheme 2. Synthesis of enones **3** and **4**.



29 The composition and stereochemistry of **3** was established by X-ray analysis. The ORTEP  
30 diagrams of **3** together with those of the remaining enones for which receiving crystalline  
31 structures were possible are presented in Figure S1 (see Supporting Information for ORTEP  
32 plots). For compound **4**, however, we were not able to grow crystals of sufficient  
33 crystallographic quality, and exhaustive NMR investigations had to be conducted to prove the  
34 structure. First of all, we had to ensure that whole abietane skeleton in **4** remained unchanged  
35 after reduction. Such changes could not be ruled out due to the reaction conditions (acidic  
36 medium, prolonged reaction time), which could favor a double bond migration or skeletal  
37 rearrangements. Comparison of 2D INADEQUATE spectra of **3** and **4** showed that none of  
38 the phenomena mentioned above occurred and both of the compounds have the same carbon  
39 atoms alignment. As can be seen in Figure 1, in both samples C7 and C8 carbon atoms are  
40 present in the "olefinic region" of <sup>13</sup>C chemical shifts (140-150 ppm) while carbons C12 and  
41  
42  
43  
44  
45  
46  
47  
48  
49  
50  
51  
52  
53  
54  
55  
56  
57  
58  
59  
60

C13 are located in the aliphatic part of spectra. Therefore, the only possibility is that enones **3** and **4** are stereoisomers which differ solely in configuration at C13.

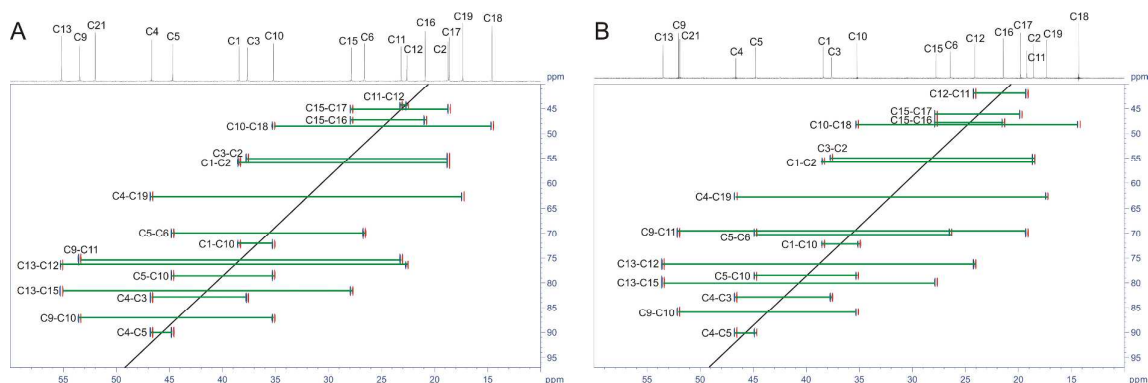


**Figure 1.** Aliphatic part of  $^{13}\text{C}$ - $^{13}\text{C}$  2D INADEQUATE spectra of **3** (A) and **4** (B) optimized for  $^1J_{^{13}\text{C}-^{13}\text{C}} = 33$  Hz. Full  $^{13}\text{C}$ - $^{13}\text{C}$  2D INADEQUATE spectra of **3** and **4** optimized for  $^1J_{^{13}\text{C}-^{13}\text{C}} = 50$  Hz are collected in the Supporting Information part together with the complete set of  $^1\text{H}$  NMR,  $^{13}\text{C}$  NMR, DEPT, 2D  $^1\text{H}$ - $^{13}\text{C}$  HSQC spectra of these enones.

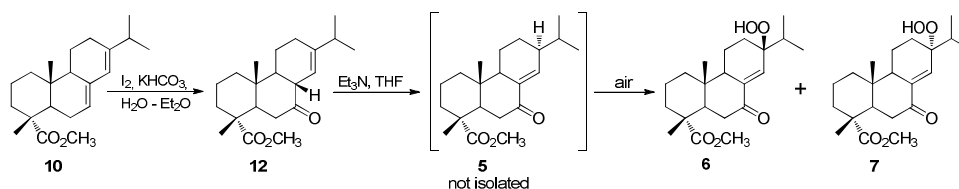
Having proven structures **3** and **4**, we must note that signals of H-C15 protons in  $^1\text{H}$  NMR and  $^1\text{H}$ - $^{13}\text{C}$  HMBC spectra are present at 2.71 ppm and 1.97-2.06 ppm (overlapped with H-C13), respectively. Such a difference equal to 0.7 ppm for very similar compounds seems to be unusual. However, the methine proton H-C15 in **3** belongs to an equatorial isopropyl group and in some conformations may lie in the plane of the carbonyl group (deshielding zone of C=O) and therefore its signal is strongly shifted downfield. In the case of **4** an axial orientation of the isopropyl group prevents planar alignment of the methine proton H-C15 together with the carbonyl group, and therefore the proton signal appears in the typical for such protons region of the spectrum.

Preparation of conjugated enones with 8(14)-en-7-one system is presented in Scheme 3. The abietic acid methyl ester **10** was oxidized to  $\beta,\gamma$ -unsaturated ketone **12** in reaction with iodine and aqueous potassium bicarbonate according to the literature procedure.<sup>11a</sup> The stereochemistry of the C8 carbon atom in **12** has been determined using single crystal X-ray

1  
2  
3  
4  
5  
6  
7  
8  
9  
10  
11  
12  
13  
14  
15  
16  
17  
18  
19  
20  
21  
22  
23  
24  
25  
26  
27  
28  
29  
30  
31  
32

diffraction analysis (Figure S11). We expected that the double bond in **12** would easily migrate in the presence of a base creating a conjugated enone **5**. In fact, when we kept the solution of **12** in THF with triethylamine for 24 hrs at room temperature, the double bond migration indeed occurred. However, the migration was instantly followed by an air oxidation at the allylic position to form two epimeric hydroperoxides **6** and **7** (Scheme 3). The same result was obtained when the reaction was carried out under argon atmosphere in a strictly deoxygenated mixture of THF and triethylamine. We conclude that the air oxidation of the allylic position in 8(14)-en-7-one derivative **5** must be fast and undergoes spontaneously at the workup stage. Therefore, preparation of a pure compound **5** seems to be difficult, if possible at all, in standard laboratory work requiring column chromatography purification.

### Scheme 3. Synthesis of enones 5-7.



A sample of a small amount of enone **5** for ECD/NMR measurements was obtained by isomerization of **12** in deoxygenated toluene in the presence of a catalytic amount of sodium *t*-butoxide followed by the separation of **5** from an unchanged **12** with the help of preparative TLC. The material washed out from the spot assigned to the conjugated enone consisted of enone **5** and freshly formed hydroperoxides **6** and **7** in a ratio 5:5:1 as it was revealed by  $^1H$  NMR spectrum (Figure 2). It must be mentioned that enone **5** differs significantly in polarity from hydroperoxides **6** and **7** in respect to TLC chromatography ( $R_f = 0.52$ ,  $0.37$  and  $0.29$  respectively, 30% ethyl acetate in hexane). Hence, it can be excluded that the enone **5** washed out from the silicagel was contaminated with **6** and **7** due to the imperfect isolation of particular spots. Detection of the moderately high concentration of hydroperoxides **6** and **7**

besides enone **5** in the same fraction confirms an exceptional susceptibility of the latter to oxidation.

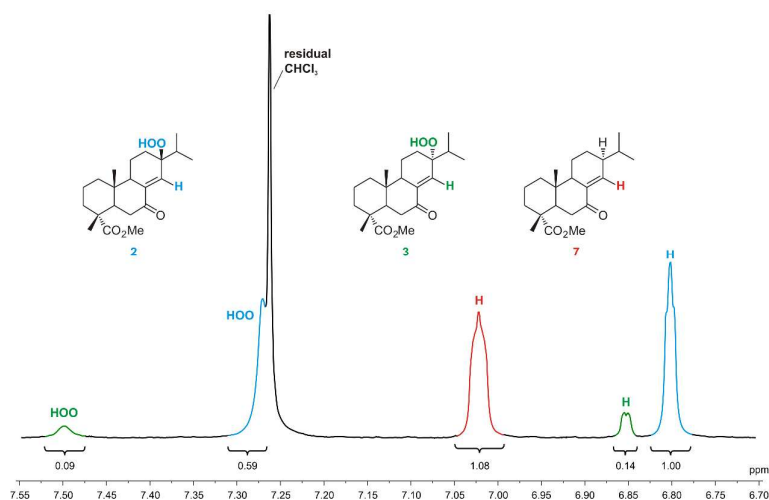


**Figure 2.** Fragment of  $^1\text{H}$  NMR spectrum of the enones **5**, **6** and **7** mixture covering the range of vinyl protons and hydroperoxide groups.

Given the extreme sensitivity of enone **5** to even trace amounts of oxygen in the reaction medium, determination of the stereochemistry at its C13 carbon atom was only possible by employing the online HPLC-ECD technique.<sup>13</sup> This method, in fact, allows recording ECD spectra during the HPLC separation without the need to isolate and purify the components of the mixture tested. By using the silica gel Kromasil® Si100, 5  $\mu\text{m}$ , 25x0.4 cm mm column and the mixture of MTBE and hexane (isocratic 1:9 mobile phase for 10 min following injection, then run linear gradient to 2:8 in 10 min, then constant 2:8, v/v) we were able to separate all three enones (Figure 3A). The retention time of the first chiral compound, *i.e.*, enone **5** (red peak, the first negative in ECD chromatogram), was 13 min. The next two epimeric hydroperoxides **6** and **7** (blue peak and green peak, respectively) with retention times 27 and 43 min were also negative. The use of stop flow mode enabled recording the ECD spectrum of enone **5** in the entire diagnostic range, *i.e.*, 220-450 nm. Comparison of the computed spectra for 13*R* and 13*S* epimers of **5** calculated after geometry optimization at the B3LYP/TZVP/PCM level of theory and the Boltzmann averaging of all populated conformers

pointed to the 13*S* AC (Figure 3B). To prevent drawing erroneous conclusions and increase the level of confidence of the stereochemical assignment, we performed QC calculations at different levels of theory. Theoretical predictions resulting from these calculations lead to the same result (Figure S2), and thus the 13*S* AC of enone **5** can be regarded as established with a high degree of certainty. The details of the calculations are presented in the experimental section as well as in the following part discussing the results of circular dichroism.

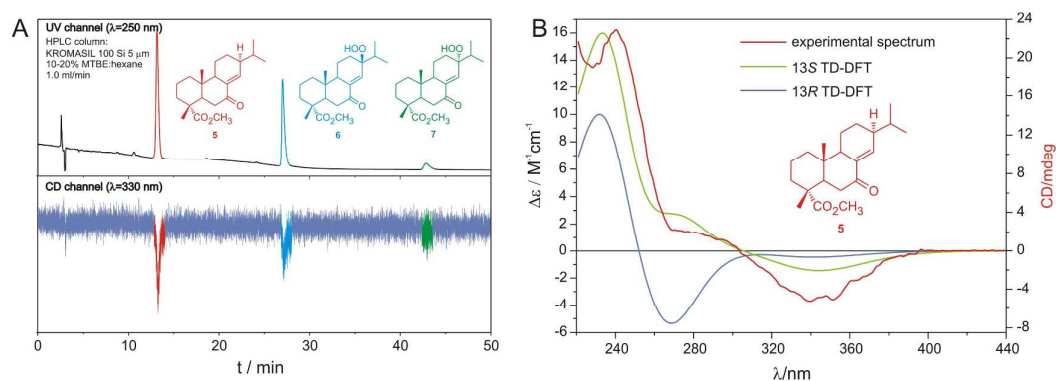
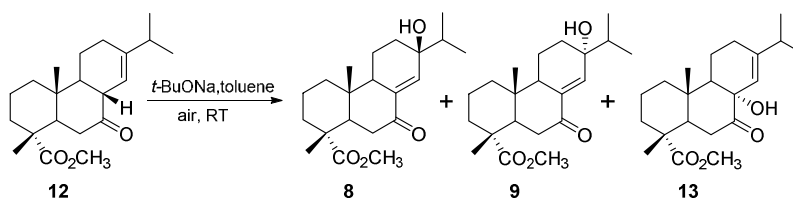


**Figure 3.** A: The UV (top) and ECD (bottom) chromatogram of **5-7** mixture on Kromasil<sup>®</sup> (Si100, 5  $\mu$ m) column, eluent 10-20 % MTBE in hexane, flow 1 mL/min, UV detection at 250 nm, ECD detection at 330 nm; B: on-line recorded ECD spectrum of enone **5** (red line) with the computed at B3LYP/TZVP/PCM(CH<sub>3</sub>CN) level of theory spectra of its 13*R* (blue line) and 13*S* (green line) epimers.

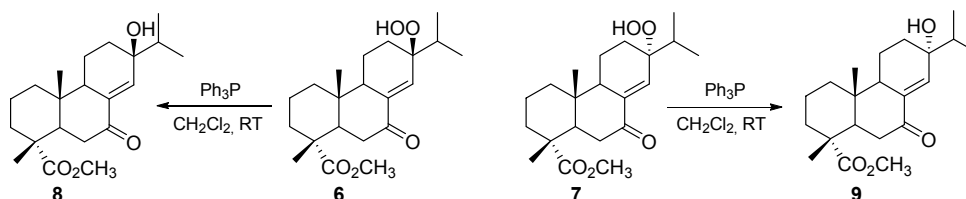
Interestingly, different results were obtained when the isomerization reaction of **12** was carried out with a catalytic amount of sodium *tert*-butoxide in anhydrous toluene in an air atmosphere. In this case, the allylic oxidation also took place, but three new allylic alcohols **8**, **9**, and **13** were the products, not the hydroperoxides obtained before (Scheme 4). Alcohols **8**, **9**, and **13** have been obtained in the yield 26:11:34, respectively.

#### Scheme 4. Synthesis of enones **8**, **9**, **13**.



Stereochemical assignment of hydroperoxides **6**, **7** and alcohols **8**, **9** and **13**, was accomplished with the assistance of single crystal X-ray analysis. Hydroperoxide **6** and alcohols **9** and **13** directly provided sufficient crystals for X-ray measurements (see Figure S11). Reduction of the hydroperoxide **7** with triphenylphosphine in methylene chloride afforded material identical in  $^1\text{H}$  NMR and  $^{13}\text{C}$  NMR spectra with the crystalline alcohol **9** revealing an equatorial position of the hydroperoxide group in **7**. An analogous reduction of crystalline axial hydroperoxide **6** provided material identical with alcohol **8** proving an axial orientation of its hydroxyl group (Scheme 5, Figure S11). Thus, based on the single crystal X-ray results, the AC at the C13 carbon atom in hydroperoxide **6** and alcohol **9** was directly assigned to be  $13S$ , and  $13R$  respectively, whereas the one at C8 carbon atom in  $\beta,\gamma$ -unsaturated keto alcohol **13** to be  $8S$ . Comparison of the NMR spectra of the respective reduction products led to an indirect assignment of AC in hydroperoxide **7** as  $13R$  and in alcohol **8** as  $13S$ . An independent confirmation of this assignment was provided by the full compliance of experimental and simulated ECD spectra of the corresponding alcohols and hydroperoxides, as shown in the next section, Table 1 and Supporting Information part.

#### Scheme 5. Reduction of hydroperoxides **6** and **7**.



Structures **8** and **9** have been already noted in the literature. The reported physical data for these compounds, however, were not consistent with the data recorded by us. In 1983 Cilko et

1  
2  
3 al.<sup>14</sup> described alcohol **8** as a solid of mp 189-190 °C and <sup>1</sup>H NMR (CDCl<sub>3</sub>, in his article Cilko  
4 reported only diagnostic signals)  $\delta$  = 0.70 (s, CH<sub>3</sub>), 0.88 (d,  $J$  = 7 Hz, isopropyl CH<sub>3</sub>), 0.90 (d,  
5  $J$  = 7 Hz, isopropyl CH<sub>3</sub>), 1.20 (s, CH<sub>3</sub>), 6.75 (s, vinylic H). Corresponding values observed in  
6 our laboratory for **8** stand as follows: mp not detected (oil), <sup>1</sup>H NMR (CDCl<sub>3</sub>)  $\delta$  = 0.85 (s,  
7 CH<sub>3</sub>), 0.94 (d,  $J$  = 6.9 Hz, isopropyl CH<sub>3</sub>), 0.98 (d,  $J$  = 6.9 Hz, isopropyl CH<sub>3</sub>), 1.24 (s, CH<sub>3</sub>),  
8 6.74 (s, vinylic H).

9  
10  
11 In 2013 Amato et al.<sup>15</sup> described structure **9** as one of the products of abietic acid  
12 oxidation with hydrogen peroxide in the presence of methyltrioxorhenium. The presented  
13 NMR data, however, were in strong contradiction with our results. Surprisingly, all listed <sup>1</sup>H  
14 NMR and <sup>13</sup>C NMR signals perfectly agreed with our spectra of **13**. In our opinion, therefore,  
15 it is highly plausible that the structure claimed before as **9** was in fact structurally tantamount  
16 to the unconjugated hydroxyenone **13**.

17  
18  
19 Oxidations of enones with oxygen in neutral and basic media are well-recognized  
20 processes in which hydroperoxides, epoxides, and allylic alcohols are typically formed.<sup>16</sup> Due  
21 to the erratic character of such oxidations affording plenty of products and difficulties in the  
22 prediction of the major product, these reactions attracted only marginal attention in organic  
23 synthesis. Recently, some successful attempts were undertaken to improve air allylic  
24 hydroxylations of enones by carrying out the reactions in the presence of catalytic amounts of  
25 metal oxides.<sup>16</sup> In our case, finding that air oxidation of the non-conjugated enone **12** can be  
26 easily and efficiently directed toward alcohols or hydroperoxides depending on the base used  
27 in the reaction was unexpected. A complete explanation of this phenomenon requires further  
28 experimental work which is in progress in our laboratory.

## 29 30 31 32 33 34 35 36 37 38 39 40 41 42 43 44 45 46 47 48 49 50 51 **2.2. Structure – Chiroptical Properties Relationship**

52  
53 For the evaluation of the structure – circular dichroic activity relationship, we took into  
54 account abietane  $\alpha,\beta$ -enones **2-9** of formulas presented in Chart 1 provided in the introductory  
55  
56  
57  
58  
59  
60

section. Their experimental UV-Vis and ECD data recorded in acetonitrile solution are collected in Table 1. The only exception in this respect is the enone **5** whose ECD spectrum was recorded in the stop flow mode during the HPLC separation with *on-line* ECD detection in a mixture of hexane : MTBE 9:1, as already mentioned before. Its UV-Vis spectrum was simultaneously measured in the same solvent mixture, and in the Table it is given in arbitrary units (a.u.) while ECD in mdeg.

Compounds **12** and **13** obtained during our synthesis exemplify  $\beta,\gamma$ -unsaturated ketones. Therefore, their chiroptical data as, for example, the location of ECD bands in their ECD spectra differ significantly from the other compounds analyzed. A blue shift of CE associated with the  $n-\pi^*$  transition, *i.e.*, 280 nm in enones **12** and **13** vs 350 nm in remaining enones, clearly indicates the absence of conjugation in the first two. Change of orientation of the substituent at the C8 carbon atom, *i.e.*,  $8\beta$ -H in **12** vs.  $8\alpha$ -OH in **13** without reversal of the AC associated with the formal inversion of chirality according to the CIP sequence rule, does not significantly affect the shape of ECD spectra. Signs of individual CEs are consistent, and their positions on the spectra are very similar. The AC assignment was obtained by the single crystal X-ray analysis enabling determination  $8S$  AC in both these compounds (Figure S11). Also, calculated ECD spectra agreed well with the observed ECD curves in sign and pattern, as can be seen in Figure S3 (for calculation details see below and experimental section).

**Table 1.** UV-Vis and ECD data of enones **2-9** and **12-13** recorded in acetonitrile. UV and ECD values are given in  $M^{-1}cm^{-1}$  as  $\epsilon$  ( $\lambda_{max}/nm$ ) and  $\Delta\epsilon$  ( $\lambda_{max}/nm$ ), respectively. UV-Vis and ECD data for enone **5** (for clarity marked in gray) were registered in the stop flow mode during HPLC separation in a mixture of hexane:ethyl acetate 9:1 and are given in a.u. (arbitrary units) and mdeg, respectively.

Enone	UV [ $\epsilon$ ( $\lambda_{max}$ )]			ECD [ $\Delta\epsilon$ ( $\lambda_{max}$ )]			
<b>2</b>	6580 (252.0)	73 (329.0)	+4.15 (193.5)		+4.78 (249.5)	-0.03 (302.0)	+0.08 (341.0)
<b>3</b>	6740 (248.5)	36 (333.0)	+1.33 (198.5)	-1.03 (220.4)	-1.08 (231.6)	+0.72 (263.0)	+0.45 (337.0)
<b>4</b>	6970 (244.0)	68 (333.0)		-1.95 (220.0)	-3.15 (241.5)	+0.02 (273.2)	-0.90 (326.0)
<b>5</b>	1.429 (243.5)	0.004 (322.0)			+23.0 (250.0)	+2.00 (280.0)	-4.80 (345.0)
<b>6</b>	8430 (242.5)	44 (326.0)		+5.96 (205.0)	+5.57 (241.0)		-0.77 (346.0)
<b>7</b>	7510 (245.0)	50 (325.0)	+5.15 (191.0)	+7.57 (208.5)	-6.01 (252.5)		-0.81 (339.0)
<b>8</b>	8760 (244.5)	82 (323.5)		+4.24 (204.5)	+4.15 (239.0)		-0.64 (348.5)

<b>9</b>	7190 (247.0)	55 (326.0)		+7.37 (204.0)	-2.51 (255.0)		-1.01 (335.0)
<b>12</b>	762 (234.0)	113 (286.0)	+9.5 (188.5)	+4.43 (216.5)			-1.29 (289.0)
<b>13</b>	2580 (220.5)	105 (281.5)	+11.7 (185.0)	+2.52 (222.5)			-4.55 (288.0)

The UV-Vis spectra of  $\alpha,\beta$ -unsaturated ketones **2-9** display two well-resolved bands arising at around 330 and 240 nm with an intensity characteristic for the corresponding  $n-\pi^*$  and  $\pi-\pi^*$  electronic transitions, respectively. As can be seen in Table 1, in their ECD spectra there are up to four bands visible within the spectral range of 190-360 nm. The ECD spectra of hydroperoxides **6** and **7** are very similar in sign and pattern to those of their hydroxyl counterparts **8** and **9** (Figure S4) thus demonstrating an equivalent effect of both these substituents on the spectra. This is a consequence of a comparable electronic system in both hydroperoxide and hydroxyl groups. Due to the small differences in the spectra, further discussion of these compounds will be considered together as hydroxyl derivatives **8** and **9**.

Regarding the spectra pattern and CEs signs, the ECD spectra of  $\alpha,\beta$ -enones **4**, and **6-9** show similar profiles with a negative  $n-\pi^*$  CE of comparable intensities of about  $\Delta\epsilon \approx 1$ . Two remaining enones. *i.e.*, **2** and **3**, exhibit a positive  $n-\pi^*$  CE of very low and low intensity, respectively. In their majority, the enones studied are homohelical as the enone torsion angle  $\omega$  and the ene torsion angle  $\tau$  defined as  $C/H-C=C-C(=O)$ , where C/H is *syn* to the  $C-C(=O)$  bond,<sup>17</sup> are of the same sign (Table 2). Also worth mentioning is the small size of the  $\tau$  angle in solution, thus mining only a minimal twist of the enone double bond and therefore practically not affecting the ECD spectra.

**Table 2.** The enone torsion angle  $\omega$  defined as  $C=C-C(=O)$ , the ene torsion angle  $\tau$ , and the signs of experimental  $n-\pi^*$  Cotton effects measured in acetonitrile compared with the same CE signs simulated at different levels of theory. The ene torsion angle  $\tau$  is defined as  $C/H-C=C-C(=O)$ , where C/H(R) is *syn* to the  $C-C(=O)$  bond, for the enones of interest given for lowest optimized energy conformations and for crystallographic samples where available.

Enone	Level of theory / X-ray data	$\omega$	$\tau$	$n-\pi^*$ CE sign	
				Exp.	Theory
<b>2</b>	B3LYP/TZVP/PCM(CH <sub>3</sub> CN)	-11.4	-0.2	-/+	+
<b>3</b>	X-ray	+26.6	+0.5		
	B3LYP/aug-cc-pVDZ/PCM(CH <sub>3</sub> CN)	+16.6	+1.6	+	+

	CAM-B3LYP/aug-cc-pVDZ/PCM(CH <sub>3</sub> CN)	+18.0	+1.4	+	+
	B3LYP/TZVP/PCM(CH <sub>3</sub> CN)	+17.1	+1.5	+	-
	CAM-B3LYP/TZVP/PCM(CH <sub>3</sub> CN)	+18.3	+1.3	+	-
<b>4</b>	X-ray	+18.8	-4.1		
	B3LYP/aug-cc-pVDZ/PCM(CH <sub>3</sub> CN)	+28.5	+1.9	-	-
	CAM-B3LYP/aug-cc-pVDZ/PCM(CH <sub>3</sub> CN)	+28.8	+1.5	-	-
	B3LYP/TZVP/PCM(CH <sub>3</sub> CN)	+27.0	+2.0	-	-
	CAM-B3LYP/TZVP/PCM(CH <sub>3</sub> CN)	+27.3	+1.6	-	-
<b>5</b>	B3LYP/aug-cc-pVDZ/PCM(CH <sub>3</sub> CN)	-14.8	-0.4	-	-
	CAM-B3LYP/aug-cc-pVDZ/PCM(CH <sub>3</sub> CN)	-14.9	-0.3		
	B3LYP/TZVP/PCM(CH <sub>3</sub> CN)	-15.2	-0.7	-	-
	CAM-B3LYP/TZVP/PCM(CH <sub>3</sub> CN)	-15.7	-0.5	-	-
<b>6</b>	X-ray	-13.7	+7.1		
	B3LYP/aug-cc-pVDZ/PCM(CH <sub>3</sub> CN)	-13.1	-1.4	-	-
<b>7</b>	B3LYP/aug-cc-pVDZ/PCM(CH <sub>3</sub> CN)	-17.3	+0.3	-	-
<b>8</b>	B3LYP/aug-cc-pVDZ/PCM(CH <sub>3</sub> CN)	-10.5	-2.2	-	-
<b>9</b>	X-ray	-8.0	-3.0		
	B3LYP/aug-cc-pVDZ/PCM(CH <sub>3</sub> CN)	-18.2	+0.5	-	-

In this context, the intrinsic helicity of the enone chromophore expressed by angle  $\omega$  should remain a decisive factor for the sign of  $n-\pi^*$  CE by assuming that the external dissymmetric perturbations have only a limited impact on the optical activity of enones as required by the Kirk rule.<sup>4b</sup> At first glance, this seems to be true as the investigated enones exhibit a positive/negative CE in the  $n-\pi^*$  transition spectral range for a positive/negative twist of the enone system. The only exceptions in this regard are enones **2** and **4** having opposite signs of angle  $\omega$  and  $n-\pi^*$  CE. Moreover, the data from Table 2 demonstrate that the second principle of Kirk's rule, concerning opposing signs of  $n-\pi^*$  and  $\pi-\pi^*$  CEs, is not fulfilled for **2**, **4**, **7**, and **9**. Even taking into account the bisignate character of  $n-\pi^*$  CE of enone **2**, it can be stated that Kirk's rule does not cover all enones investigated. Therefore, to achieve a more in-depth insight into incompatibilities mentioned above and to be able to draw more definite conclusions we have decided to expand our dichroic experiments on solvent dependency studies and variable temperature measurements in both polar and non-polar solvents.

For all the enones, quantum chemical calculations were implemented to support experimental data. At the outset, the conformational analysis was done with CONFLEX 7<sup>18</sup> and ComputeVOA v. 1.0<sup>19</sup> programs using MMFF94s<sup>20</sup> and MMFF94<sup>20-21</sup> force fields, respectively (for details see the experimental section). For enone **2**, two identical sets of five conformers in an energy window of 5 kcal/mol resulted in both force fields. For further analysis, contributions to the overall spectra of all conformers received were taken into account. The comparison of experimental and Boltzmann averaged ECD spectra showed good agreement with the isomer of 13*S* absolute configuration (Figure 4). To a similar conclusion led the analysis of VCD spectra based on the same five conformers. This way, *i.e.*, on the grounds of two independent chiroptical methods, the AC of hydroxyenone **2** has been confirmed as consistent with the literature data.<sup>9b</sup>

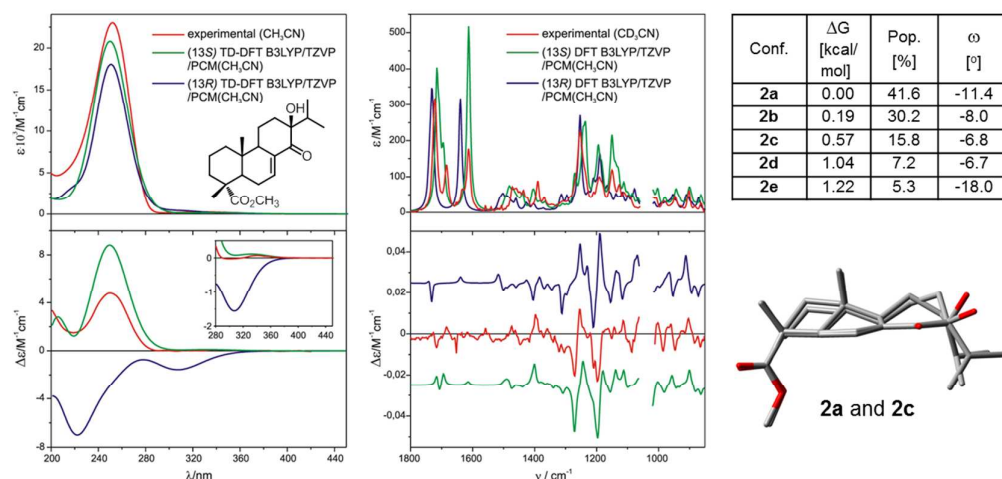


**Figure 4.** The experimental and simulated ECD (left) and VCD (middle) spectra of hydroxyenone **2** averaged with the Boltzmann distribution at B3LYP/TZVP/PCM(CH<sub>3</sub>CN) level of theory (insert shows the n- $\pi^*$  range of ECD spectra recorded in acetonitrile); Right top: Differences in Gibbs energy ( $\Delta G$ ), population (Pop.), and enone torsion angle values ( $\omega$ ) for individual conformers of hydroxyenone **2**; Right bottom: overlay of conformers **2a** and **2c** showing structural differences within the cyclohexanone ring and substituents on carbon C13

in two of the three lowest energy conformers. For remaining conformers see Supporting Information section.

The ECD spectra of enones **3** and **4** were further analyzed to confirm the previously assigned AC at the C13 carbon atom. As it turned out, these spectra differ in the sign of the  $n-\pi^*$  CE thus indicating a different AC as expected. Comparison of the experimental and computed at the B3LYP/aug-cc-pVDZ level of theory spectra, considering the Boltzmann averaging from all populated above 1% conformers in combination with previous data from X-ray for **3** and NMR for **4**, confirmed AC to be 13*R* and 13*S* respectively (Figure 5). Nonetheless, the experimental and simulated spectra show a lack of satisfactory compliance, particularly pronounced for the enone **3** in the  $\pi-\pi^*$  range. Moreover, in both of these enones, the computed spectra do not accurately reflect the positive CE present at around 260 nm with varying intensity for **3** and **4**. The solvent change also does not affect the shape of the ECD curves of enone **3**. In the case of enone **4**, however, this small positive CE at  $\sim 260$  nm observed in hexane, acetonitrile, and chloroform disappears in polar solvents such as methanol and trifluoroethanol (Figure 5).

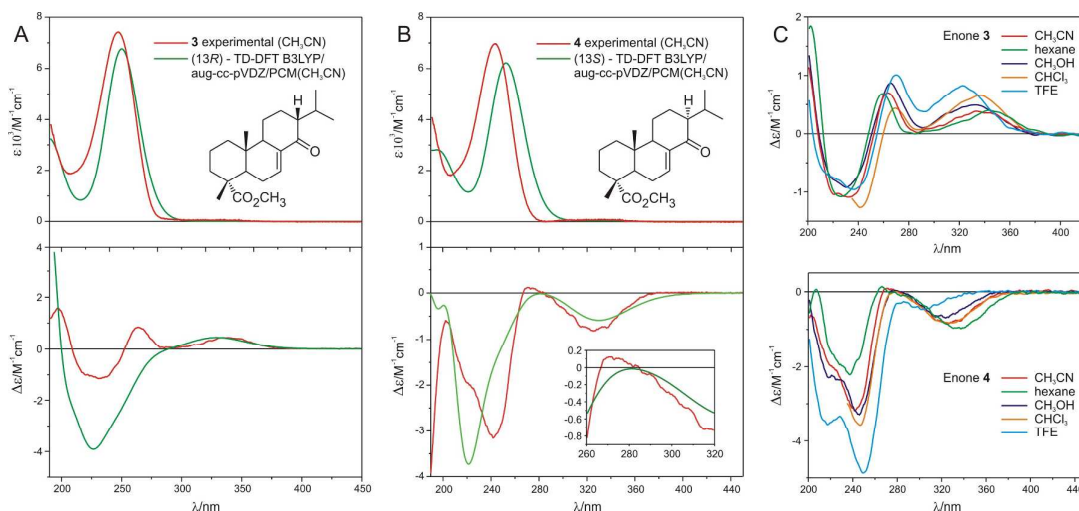


**Figure 5.** Comparison of computed at the B3LYP/aug-cc-pVDZ/PCM(CH<sub>3</sub>CN) level of theory UV/Vis and ECD spectra of enones **3** (A) and **4** (B) obtained as a population-weighted

1  
2  
3 sum of the calculated spectra of individual conformers with experimental spectra recorded in  
4 CH<sub>3</sub>CN. Insert in ECD part B shows a comparison of experimental and computed ECD  
5 spectra of the enone **4** in the range of an n- $\pi^*$  transition indicating lack of positive fragment in  
6 the calculation; Panel C: ECD spectra of **3** (top) and **4** (bottom) measured in various solvents  
7 (TFE = trifluoroethanol).  
8  
9  
10  
11  
12

13  
14 Having certainty about maintaining of entire carbon skeleton, we decided to check the  
15 reliability of our ECD calculations by ensuring that non-satisfactory accuracy between  
16 experiment and theory does not result from the use of an inadequate level of theory.  
17 Therefore, for computational purposes, we applied various combinations of hybrid functionals  
18 (CAM-B3LYP,<sup>22</sup> B3LYP<sup>23</sup>) and basis sets (TZVP,<sup>24</sup> aug-cc-pVDZ<sup>25</sup>) preceded by a thorough  
19 conformational search run with force fields MMFF94s<sup>20</sup> implemented to Conflex<sup>18</sup> and  
20 MMFF<sup>26</sup> to Spartan.<sup>27</sup> This step was followed by geometry re-optimization of all energy  
21 minima found by DFT with regard to the solvent effect of acetonitrile by applying continuum  
22 solvation model (PCM).<sup>28</sup> Yet, improving the experiment compliance with theory could not  
23 be achieved. In contrast to the UV-Vis spectra which are well reproducible irrespective of the  
24 level of theory, in ECD spectra even the sign of n- $\pi^*$  CE becomes inverted depending on the  
25 level used, as can be seen in Figure 6A. Regardless of this, the calculations have shown that  
26 the sign of the CE at ~320 nm is sensitive to subtle structural factors, such as, the  
27 conformation of the isopropyl group at C13 which significantly affects the value of the  
28 rotational strength. Such an impact is particularly pronounced in the case of enone **3**. On the  
29 other hand, the lack of good agreement between experiment and computation is not too  
30 surprising given the small intensities of the considered bands.<sup>29</sup>  
31  
32  
33  
34  
35  
36  
37  
38  
39  
40  
41  
42  
43  
44  
45  
46  
47  
48  
49  
50  
51  
52  
53  
54  
55  
56  
57  
58  
59  
60

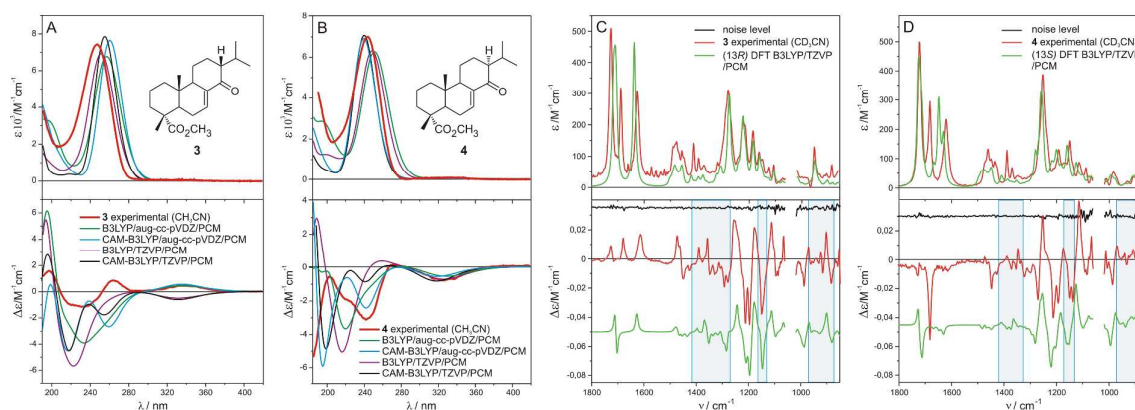


**Figure 6.** Comparison of experimental and computed UV-Vis (top) and ECD (bottom) spectra at various levels of theory of enones **3** (A) and **4** (B); Comparison of computed IR (top) and VCD (bottom) spectra of enones **3** (C) and **4** (D) obtained as a population-weighted sum of the calculated spectra of individual conformers with experimental spectra.

Given the inconsistencies between ECD experiment and theory, we decided to apply a quantitative approach to compare experimental and calculated spectra of enones **3** and **4**, and *ipso facto* obtain an answer to the question of how trustworthy assignment based on ECD is. To accomplish this, we took advantage of the similarity analysis implemented to the SpecDis 1.70 software.<sup>30</sup> For clarity and brevity, we show here only results based on spectra calculated at the B3LYP/TZVP/PCM(CH<sub>3</sub>CN) level of theory. Table 3 illustrates the similarity factors (SF) obtained using relevant calculated and experimental data for the best numerical level of matching between them. Moreover, for each comparison, the UV shift correction factors, band broadening and enantiomeric similarity index (ESI) are shown.

**Table 3.** A numerical analysis of the comparison between experimental and computed spectra for **3** and **4** using the SpecDis.<sup>30</sup> Note: the experimental and calculated ECD/UV-Vis spectra at B3LYP/TZVP/PCM(CH<sub>3</sub>CN) level of theory were fit in the range from 195 nm to 400 nm by using UV shift correction ranging from -30 to +30 nm, and bandwidth values from 0.1 to 0.5 eV. Abbreviations used: SF = similarity factor index; ESI = enantiomeric similarity index (the highest value found using criteria mentioned above) defined as the difference between SF of a compound and SF of its enantiomer.

Enone	UV shift (nm)	Bandwidth (eV)	SF	SF for enantiomer	ESI
<b>3</b>	-5	0.43	0.853	0.115	0.738

<b>4</b>	-6	0.34	0.923	0.031	0.892
----------	----	------	-------	-------	-------

From Table 3 it becomes clear that for **4** the ESI value of ~89% is large enough to suggest high credibility of 13*S* configurational assignment. On the other hand, ESI of epimer **3** amounting ~74%, so being 17% lower than that of **4**, can nevertheless be considered as indicative of 13*R* absolute configuration. However, to obtain a reliable assignment of the absolute configuration of enones **3** and **4** on the CD basis, we used VCD again. The agreement between experimental and simulated VCD spectra obtained for the same set of conformers as for ECD support predetermined AC (Figure 6C-D). The resulting reliability of the assignment was entirely satisfactory as the confidence level algorithm for comparing VCD experimental and theoretical spectra<sup>19a, 31</sup> was 100% for **4** in the 1500-850 cm<sup>-1</sup> range. For the 1800-850 cm<sup>-1</sup> range this algorithm was a little lower and amounted to 96%. In fact, most of the bands in experimental VCD spectra are matched by calculations in sign but some of them not perfectly in magnitude. This inaccuracy may be related to the flexibility of the molecules within the isopropyl and ester groups. Consequently, the 13*S* AC for **4**, confirmed by two independent chiroptical methods supported by NMR data can be considered as certain.

Our DFT calculations show that unlike the lowest-energy ECD band, the band at around 260 nm is not pure as, in addition to enone  $\pi$ - $\pi^*$  transition, it consists of various types of electronic excitations from the ester group at C4 and substituents on the C13 carbon atom (for details see Supporting Information section).

Polar substituents have a significant influence on the spectra through their conformational mobility and intra- or intermolecular interaction. This is particularly evident for enone **2**, whose spectra, depending on the polarity of the solvent, are almost perfect mirror images in the range of  $n$ - $\pi^*$  transition (Figure 7). Cotton effect corresponding to this transition is for nonpolar solvents such as hexane or chloroform bisignate with +/- sign sequence on going

towards lower energies. In polar solvents, however, the signs' sequence turns to the opposite which ultimately results in spectra of almost mirror image character for hexane and methanol (Figure 7). Thus, we are dealing here with a system that exhibits chirality-inversion effect dependent upon the polarity of the solvent used. It should also be noted that these calculations do not reproduce the bisignate features of the  $n-\pi^*$  band.

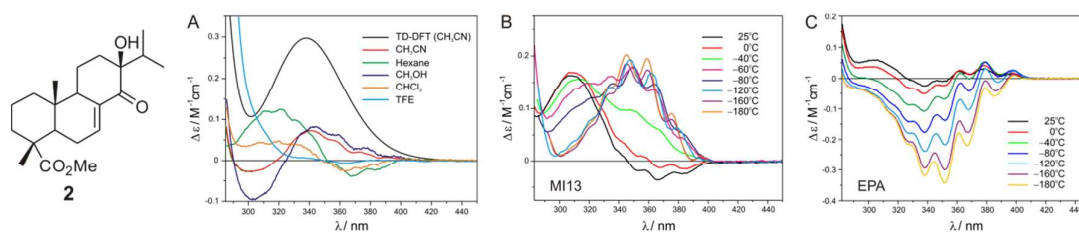


**Figure 7.** A: Experimental ECD spectra of the enone **2** presented in the range of  $n-\pi^*$  transition in various solvents together with the spectrum simulated at B3LYP/TZVP/PCM(CH<sub>3</sub>CN) level of theory; B: ECD spectra of enone **2** recorded in MI13 (methylcyclohexane/isopentane, 1:3, v/v); C: ECD spectra of enone **2** recorded in EPA (Et<sub>2</sub>O/isopentane/EtOH, 5:5:2, v/v). The symbol  $\Delta\epsilon$  denotes the difference of the molar decadic absorption coefficients of left and right circularly polarized light, and  $\lambda$  – the wavelength. The lower temperature curves have been corrected for solvent contraction.

Such a strong solvent effect on ECD spectra was also confirmed by variable temperature measurements. In a nonpolar solvent (MI13: methylcyclohexane/isopentane, 1:3, v/v) already at  $-40$  °C there is a change of bisignate  $n-\pi^*$  CE sign sequence from  $+/-$  to  $+/+$  (viewed in the direction of decreasing energy) with maxima occurring at 312 and 355 nm. Further lowering temperature to  $-80$  °C causes the formation of one positive ECD band with a maximum at 349 nm with a well-developed vibrational fine structure characteristic for enone carbonyls. This shape remains unchanged with an additional decrease in temperature to  $-180$  °C (Figure 7). In a polar solvent (EPA: Et<sub>2</sub>O/isopentane/EtOH, 5:5:2, v/v) and temperatures ranging from  $+25$  °C to  $-120$  °C,  $n-\pi^*$  CE remains bisignate ( $-/+$  sign sequence in descending energy terms) with a gradual disappearance of the very weak in intensity positive part which finally

1  
2  
3 in  $-160\text{ }^{\circ}\text{C}$  becomes purely negative. In this solvent, the fine vibrational structure within  $n\text{-}\pi^*$   
4  
5 is visible in the entire temperature range, *i.e.*, from  $+25$  to  $-180\text{ }^{\circ}\text{C}$ .  
6

7 The EPA results indicate more pronounced conformational homogeneity of the rings  
8 comprising the enone chromophore evidenced by only slight changes in the shape of the ECD  
9 curve along with the lowering of the temperature. In the nonpolar solvent MI13, in turn,  
10 lowering the temperature eliminates gradually high energy conformers from equilibrium by  
11 shifting it towards more stable conformers. In this solvent, chromophore is stabilized by  
12 intramolecular hydrogen bonding between the hydroxyl group at C13 and the enone carbonyl  
13 equaling to  $2.26\text{ \AA}$ . The presence of this H-bond with the formation of an additional five-  
14 membered ring was independently verified by IR spectroscopy dilution experiments in  $\text{CCl}_4$   
15 (Figure S5). The creation of this H-bond changes the identity of the chromophore indicating  
16 the presence of different molecular species in polar and nonpolar solvents. Consequently, we  
17 are dealing with various behaviors depending on solvent polarity ultimately resulting in  
18 differences in the spectra shapes. The most exciting conclusion from this variable temperature  
19 measurements is apparent solvent- and temperature-mediated chirality inversion, as can be  
20 clearly seen when comparing the spectra in MI13 and EPA starting from  $-120\text{ }^{\circ}\text{C}$  up to  $-180$   
21  $^{\circ}\text{C}$ .  
22  
23  
24  
25  
26  
27  
28  
29  
30  
31  
32  
33  
34  
35  
36  
37  
38  
39

40 Remaining enones, in particular **8-9** in which intramolecular interactions do not exist, do  
41 not exhibit such a spectacular dependency on solvent and temperature. The impact of various  
42 solvents differing in polarity on the ECD spectra of enones **8** and **9** is in line with  
43 expectations. This means that with increasing solvent polarity, the band corresponding to the  
44  $n\text{-}\pi^*$  transition is subjected to a hypsochromic shift and the  $\pi\text{-}\pi^*$  to a bathochromic one in  
45 accord with the polarity of the solvents, and their intensity does not show any substantial  
46 changes (Figure S6). On the other hand, measurements at variable temperatures, ranging from  
47  $+25\text{ }^{\circ}\text{C}$  to  $-180\text{ }^{\circ}\text{C}$ , performed in a polar solvent EPA ( $\text{Et}_2\text{O}/\text{isopentane}/\text{EtOH}$ , 5:5:2, v/v)  
48  
49  
50  
51  
52  
53  
54  
55  
56  
57  
58  
59  
60

result in only a slight increase in the intensity of the bands and their bathochromic shift of 10 nm in the range of  $n-\pi^*$  transition (Figure 8 C-D, top). More pronounced changes in intensity and a hypsochromic shift of 7 and 9 nm, respectively for **8** and **9**, show these enones in a nonpolar solvent MI13 (methylcyclohexane/isopentane, 1:3, v/v) at the same temperature range, *i.e.*, from +25 °C to -180 °C (Figure 8 C-D, bottom). However, these changes remain within limits accepted for compounds of relative conformational stability, as the index  $I_{-180}^{+25}$  describing the relative change of  $\Delta\varepsilon_{\max}$  in ascending temperature terms amounts to *ca.* 48% in both cases. This value indicates a greater degree of conformational freedom in a nonpolar solvent, nevertheless still points to a noticeable hindrance to an unlimited mobility.<sup>32</sup> Moreover, it indicates the lack of necessity to stabilize the rings containing the enone chromophore and substituents through hydrogen bonding or other non-covalent interactions.

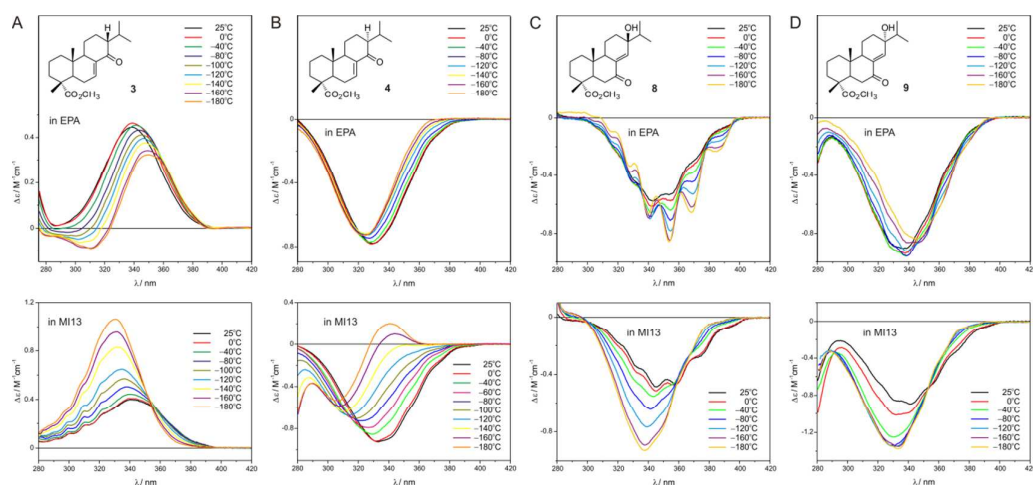


**Figure 8.** ECD spectra in the  $n-\pi^*$  range of enones **3** (A), **4** (B), **8** (C), and **9** (D) recorded top: in EPA (Et<sub>2</sub>O/isopentane/EtOH, 5:5:2, v/v), and bottom: in MI13 (methylcyclohexane/isopentane, 1:3, v/v); The symbol  $\Delta\varepsilon$  denotes the difference of the molar decadic absorption coefficients of left and right circularly polarized light, and  $\lambda$  – the wavelength. The lower temperature curves have been corrected for solvent contraction.

The variable temperature measurements further corroborated of the relative conformational stability within the skeleton including the chromophoric unit of enones **8** and **9** although, for both of them several conformers in the 10 kcal/mol energy window were

1  
2  
3 found. These conformers mainly differ in the conformation of substituents at C4 and C13.  
4  
5 They are essentially rotamers of isopropyl and ester groups as well rotamers of the hydroxyl  
6  
7 at C13 but without a hydrogen bond between the H atom of this OH group and the carbonyl  
8  
9 oxygen as evidenced by the distance between them equal to 4.56 Å in **9**.

10  
11 Lowering the measurement temperature of enones **3** and **4** results in much stronger  
12  
13 changes in both the pattern of the ECD curves and the intensity of the individual bands  
14  
15 depending on the polarity of the solvent used (Figure 8 A-B). In the EPA solvent, the ECD  
16  
17 curve of enone **3** starts already at  $-80$  °C to become bisignate reaching its final shape at  $-180$   
18  
19 °C with a minimum at 312 nm and  $\Delta\epsilon = -0.1$  followed by a maximum at 350 nm and  $\Delta\epsilon =$   
20  
21  $+0.32$  (Figure 8A, top). This result can be explained by a progressive elimination of high-  
22  
23 energy conformers from the equilibrium along with shifting this equilibrium to the most stable  
24  
25 conformer. Concurrently, the main positive band of **3** occurring in EPA at r.t at 339 nm is  
26  
27 subjected to a bathochromic shift by 11 nm. In this case, such a shift means that the most  
28  
29 stable conformation was frozen out at the lowest temperature or at least has reached a highest  
30  
31 possible population. In the case of enone **4**, however, lowering the temperature causes solely a  
32  
33 gradual intensity increase of the  $n-\pi^*$  band, in line with the expected shift of equilibrium  
34  
35 towards more stable conformations. On the contrary, in the MI13 case (MI13:  
36  
37 methylcyclohexane/isopentane, 1:3, v/v) a hypsochromic shift in the  $\lambda_{\max}$  of the  $n-\pi^*$  CEs,  
38  
39 *i.e.*,  $\Delta\lambda_{\max}$ , equaling to 12 nm and 27 nm for enones **3** and **4**, respectively, occurs with  
40  
41 decreasing temperature (Figure 8A-B, bottom). It is accompanied, as expected, by an increase  
42  
43 in intensity along with a decrease in temperature. In this nonpolar solvent, the most significant  
44  
45 changes in the shape of temperature-dependent ECD curves are observed for enone **4**. In the  
46  
47 temperature range of  $+25$  to  $-140$  °C, the hypsochromic shift of the  $n-\pi^*$  transition from 333  
48  
49 nm to 313 nm is accompanied by a gradual intensity decrease of the main negative band.  
50  
51 Further lowering of temperature to  $-160$  °C changes the shape of the curve to bisignate with a  
52  
53  
54  
55  
56  
57  
58  
59  
60

1  
2  
3 minimum at 309 nm and maximum at 348 nm indicating the presence of different conformers  
4  
5 in the equilibrium. An additional decrease of the temperature to  $-180\text{ }^{\circ}\text{C}$  shifts the  
6  
7 equilibrium toward the conformer characterized by a positive CE causing the positive part to  
8  
9 become much more pronounced at the expense of the negative one.  
10

11 The usually observed increase of intensity of ECD bands at a lower temperature is on  
12  
13 account of greater conformational homogeneity favoring the most stable conformers and a  
14  
15 shift of some maxima with decreasing temperatures can be attributed to the solute-solvent  
16  
17 interaction. This interaction, referred to as solvatochromic effect and related to the  
18  
19 dependency of absorption spectra on solvent polarity, causes the observed variations in the  
20  
21 position, intensity, and pattern of the absorption spectra. In consequence, experimentally  
22  
23 established directions and magnitudes of solvatochromic shifts are applicable for the  
24  
25 determination of the nature of electronic transition, and the estimation of dipole moments in  
26  
27 the ground and excited states.<sup>33</sup>  
28  
29

## 30 31 **CONCLUSION**

32  
33 In this paper, the synthesis of a series of abietane enones serving as model compounds for  
34  
35 chiroptical considerations has been described. We have demonstrated that for reliable  
36  
37 stereochemical conclusions to be achieved a combination of at least two different chiroptical  
38  
39 methods, *e.g.*, ECD and VCD, supported by calculations, is necessary. Such an approach  
40  
41 prevents drawing erroneous conclusions and simultaneously increases the confidence level of  
42  
43 the achieved assignment by analysis of the results in respect of electronic transitions.  
44  
45 Furthermore, the inclusion in the calculations of solvent polarity, which affects the electronic  
46  
47 structure of the solute, additionally stresses the importance of the role it plays in the case of  
48  
49 the enones tested. Thus, applying solvents of different polarity or H-bond/non-H-bond  
50  
51 competitive, and variable-temperature ECD measurements enabled us to examine their impact  
52  
53 on resulting environment change. Consequently, such an approach based on compatibility  
54  
55  
56  
57  
58  
59  
60

1  
2  
3 with the experiment allowed for the circumvention of possible errors caused by the choice of  
4 a functional and/or negligence of solvent effects. At least for enone **2**, we were able to  
5 demonstrate a relatively rare phenomenon of chirality inversion resulting in practically perfect  
6 mirror image ECD spectra, depending on both solvent and temperature applied.  
7  
8  
9

10  
11 As shown in the present study, experimental data supported by theoretical estimations  
12 resulting from the QC calculations offer an improved and reliable analysis of spectroscopic  
13 properties (position of the absorption band, molar extinction coefficient, and band shape) of a  
14 series of abietane enones. The results obtained *ipso facto* encourage a much more extensive  
15 use of chiroptical spectroscopy due to its effectiveness and credibility. In particular,  
16 application of dichroic methods for the determination of the AC is relevant in cases where  
17 other techniques, including X-ray crystallography, fail, are not applicable or give inconclusive  
18 results. For instance, the structure determination of the extremely sensitive to oxidation enone  
19 **5** became possible by employing the *on-line* HPLC-CD technique supported by calculations.  
20 Thus, the final finding of this work is to demonstrate the vital role of chiroptical methods in  
21 determining molecular structure.  
22  
23  
24  
25  
26  
27  
28  
29  
30  
31  
32  
33

## 34 35 **EXPERIMENTAL SECTION**

### 36 37 **General Techniques**

38  
39 All solvents were dried and distilled before use. All reactions were monitored by thin-  
40 layer chromatography using aluminum-backed silica gel plates 60 F<sub>254</sub>; visualization was  
41 accomplished with UV light and/or staining with 50% H<sub>2</sub>SO<sub>4</sub>. Standard flash chromatography  
42 procedures were followed using silica gel with particle size 40-63 μm. Melting points were  
43 recorded in a melting point stage and are not corrected. Optical rotation was measured in  
44 CHCl<sub>3</sub> solutions at ambient temperature and is quoted in units of 10<sup>-1</sup> deg cm<sup>2</sup> g<sup>-1</sup>. FT-IR  
45 spectra were recorded on an FT-IR spectrophotometer for KBr pellets or films or examined  
46 directly in the solid or liquid state without further preparation with Universal Attenuated Total  
47  
48  
49  
50  
51  
52  
53  
54  
55  
56  
57  
58  
59  
60

1  
2  
3 Reflectance (ATR) accessory in an FT-IR spectrophotometer.  $^1\text{H}$  NMR spectra were recorded  
4 at 400, 500 or 600 MHz and  $^{13}\text{C}$  NMR at 125 and 150 MHz using  $\text{CDCl}_3$  or  $\text{C}_6\text{D}_6$  as solvents  
5 and TMS as internal standard and are reported as  $\delta$  values (ppm) relative to residual  $\text{CHCl}_3$   
6 signal  $\delta$  H (7.26 ppm) and  $\text{CDCl}_3$   $\delta$  C (77.16 ppm), respectively.  $^{13}\text{C}$ - $^{13}\text{C}$  2D INADEQUATE  
7 spectra were recorded in concentration *ca.* 200 mg/400  $\mu\text{L}$   $\text{C}_6\text{D}_6$ .  
8  
9  
10  
11  
12

13  
14 Mass spectra (MS) were obtained with magnetic sector mass spectrometer equipped with  
15 an electron impact (EI) ion source and the EBE double focusing geometry mass analyzer at 70  
16 eV. The instrument was controlled and recorded data were processed using MassLynx 4.1  
17 software package. Electrospray ionization (ESI) experiments were performed on a mass  
18 spectrometer equipped with an electrospray ion source and q-TOF type mass analyzer under  
19 normal conditions. PFK solution was used as a calibrant for HRMS measurements. The  
20 instrument was controlled and recorded data were processed using MassLynx V4.1 software  
21 package. UV and ECD spectra of abietic enones **2–9** and **12–13** were measured essentially in  
22 acetonitrile. In selected cases, however, they were also measured in chloroform, methanol,  
23 hexane or 2,2,2-trifluoroethanol to investigate the effect of solvent on the spectrum. Spectra  
24 were recorded between 180–500 nm at room temperature using solutions with concentrations  
25 in the range  $4.6 \times 10^{-4}$  to  $2.6 \times 10^{-3}$  M, in quartz cells with path length 0.02, 0.1, 0.2, 0.5, 1 or  
26 2 cm. All spectra were recorded using 100 nm/min scanning speed, a step size of 0.2 nm, a  
27 bandwidth of 1 nm, a response time of 0.5 sec, and an accumulation of 5 scans. The spectra  
28 were background corrected.  
29  
30  
31  
32  
33  
34  
35  
36  
37  
38  
39  
40  
41  
42  
43  
44  
45

46 Low-temperature ECD measurements of **2**, **3**, **4**, **8**, and **9** were performed in the  
47 temperature range 298 – 93 K in a solution of MI13 (methylcyclohexane/isopentane, 1:3, by  
48 vol.) and EPA ( $\text{Et}_2\text{O}$ /isopentane/ $\text{EtOH}$ , 5:5:2, by vol.) as solvents. The solutions with  
49 concentrations in the range from  $1.8 \times 10^{-3}$  to  $6.7 \times 10^{-3}$  M were measured between 280  
50 – 450 nm in 1 cm quartz cell. Baseline correction was achieved by subtracting the spectrum of  
51  
52  
53  
54  
55  
56  
57  
58  
59  
60

1  
2  
3 a reference solvent obtained under the same conditions. All spectra were normalized to  $\Delta\epsilon$   
4  
5 using volume correction for MII3 and EPA.  
6

7 The VCD and IR spectra of **2-4**, **9** and **11** were measured with  $4\text{ cm}^{-1}$  resolution using  
8  
9  $\text{CD}_3\text{CN}$  as a solvent. The FT-VCD spectrometer was equipped with dual sources and dual  
10  
11 PEM (Photoelastic Modulator) technology. A solution with concentrations in the range 0.12  
12  
13 M to 0.17 M was measured in a  $\text{BaF}_2$  cell with a path length of  $100\text{ }\mu\text{m}$  (**3** and **9**) or  $102\text{ }\mu\text{m}$   
14  
15 (**2**) assembled in a rotating holder ( $14\text{ cycle}^{-1}$ ). The ZnSe PEM of the instrument was  
16  
17 optimized at  $1400\text{ cm}^{-1}$ . The spectra were measured from 5 to 12 hr to find the best signal-to-  
18  
19 noise ratio. Baseline correction was achieved by subtracting the spectrum of a solvent  
20  
21 obtained under the same conditions.  
22  
23

24 Single crystal X-ray diffraction measurements for **3**, **6**, **9**, **12** and **13** were carried out at 100  
25  
26 K with graphite monochromated  $\text{Cu K}\alpha$  radiation ( $1.54184\text{ }\text{\AA}$ ). All non-hydrogen atoms were  
27  
28 refined as anisotropic while hydrogen atoms were placed in calculated positions and refined in  
29  
30 riding mode. The data reduction was made by using the CrysAlisPRO<sup>34</sup> software. The  
31  
32 structures were solved by direct methods and refined on F2 by Full-Matrix least-squares by  
33  
34 using SHELXS97 and SHELXL97.<sup>35</sup> Crystallographic data of **3**, **6**, **9**, **12** and **13** reported here  
35  
36 have been deposited with the Cambridge Crystallographic Data Centre (Deposition No.  
37  
38 CCDC 1483005 for **3**, 1467004 for **6**, 1467005 for **9**, 1486042 for **12**, and 1467003 for **13**).  
39  
40 These data can be obtained free of charge via [www.ccdc.cam.ac.uk/data\\_request/cif](http://www.ccdc.cam.ac.uk/data_request/cif).  
41  
42  
43

#### 44 **Computational details**

45  
46 Conformational search for enones under study was done using ComputeVOA<sup>TM19a</sup>  
47  
48 CONFLEX 7<sup>18</sup> and/or SPARTAN 14<sup>27</sup> programs with MMFF94,<sup>21</sup> MMFF94s<sup>20</sup> and MMFF<sup>26</sup>  
49  
50 force fields within  $10\text{ kcal mol}^{-1}$  energy windows. Subsequently, all structures were submitted  
51  
52 to the Gaussian 09<sup>36</sup> program for optimisation at the DFT level using the  
53  
54 B3LYP/TZVP/PCM( $\text{CH}_3\text{CN}$ ), B3LYP/aug-cc-pVDZ/PCM( $\text{CH}_3\text{CN}$ ), CAM-B3LYP/TZVP/  
55  
56  
57  
58  
59  
60

1  
2  
3 PCM(CH<sub>3</sub>CN) or CAM-B3LYP/aug-cc-pVDZ/PCM(CH<sub>3</sub>CN) level of theory. All conformers  
4  
5 were confirmed to contain no imaginary frequencies. Then, final low-energy structures (0 – 5  
6  
7 kcal mol<sup>-1</sup>) were used for TDDFT simulation of UV and ECD spectra using the same level of  
8  
9 theory and the polarisable continuum model (PCM) for CH<sub>3</sub>CN. Rotatory strengths were  
10  
11 calculated using both length and velocity representations; the differences between them were  
12  
13 less than 5%, and for this reason, only the velocity representations ( $R_{vel}$ ) were taken into  
14  
15 account.  
16

17  
18 The UV and ECD spectra were simulated by overlapping Gaussian functions for each  
19  
20 transition. The final spectrum was obtained by Boltzmann averaging (T= 298 K) according to  
21  
22 the population percentages of individual conformers based on the relative Gibbs energies  
23  
24 calculated at the same level as the DFT optimisation. A Gaussian band-shape was applied  
25  
26 with 0.35 eV as a half-height width. Before comparing the predicted and experimental ECD  
27  
28 spectra, the agreement of experimental and calculated UV/Vis spectra was verified as their  
29  
30 conformity is a prerequisite for analyzing the corresponding ECD spectra.<sup>37</sup>  
31  
32

33 IR and VCD calculations were carried out in Gaussian 09<sup>36</sup> for the same conformers as the  
34  
35 UV and ECD spectra at the B3LYP/TZVP/PCM(CH<sub>3</sub>CN) level of theory. The final spectrum  
36  
37 was obtained by Boltzmann averaging (T=298 K) according to the population percentages of  
38  
39 the individual conformers based on the relative Gibbs energies calculated at the same level of  
40  
41 theory. To compare experimental and Boltzmann spectra and to determine the confidence  
42  
43 level, CompareVOA<sup>31</sup> program was used.  
44  
45

#### 46 **Purification of abietic acid (1).**

##### 47 a) Preparation of isopentylammonium abietate

48  
49 Isopentylamine (13 ml, 0.11 mol) was added to a solution of commercial abietic acid (30 g,  
50  
51 0.1 mol) in ethanol (55 mL) and the mixture was refluxed for 15 min. Then the hot mixture  
52  
53 was diluted with water (45 mL) and allowed to stand overnight at room temperature. The  
54  
55  
56  
57  
58  
59  
60

1  
2  
3 collected crystals (27 g) of amine salt was filtered off and recrystallized from ethanol (40 mL)  
4 and water (40 mL). 24 g (62% overall yield) of pure isopentylammonium abietate was  
5 obtained as colorless crystals, mp 107–109 °C.  $[\alpha]_D^{22} -66.5$  (c 0.6, CHCl<sub>3</sub>). <sup>1</sup>H NMR (500  
6 MHz, C<sub>6</sub>D<sub>6</sub>): δ 7.39 (br s, 3H), 5.74 (s, 1H), 5.35 (br s, 1H), 2.77–2.74 (m, 2H), 2.21 (septet, *J*  
7 = 6.7 Hz, 1H), 2.11–1.98 (m, 4H), 1.93–1.68 (m, 5H), 1.64–1.46 (m, 6H), 1.19 (s, 3H), 1.25–  
8 1.08 (m, 2H), 1.00 (d, *J* = 6.7 Hz, 3H), 0.99 (d, *J* = 6.8 Hz, 3H), 0.87 (d, *J* = 6.4 Hz, 6H), 0.82  
9 (s, 3H). <sup>13</sup>C NMR (125 MHz, C<sub>6</sub>D<sub>6</sub>): δ 184.9, 144.9, 135.6, 122.6, 121.0, 51.2, 46.8, 45.5,  
10 38.7, 38.3, 38.0, 37.6, 34.9, 34.5, 27.5, 26.0, 25.9, 22.5, 22.4, 22.3, 21.4, 20.8, 18.5, 17.5,  
11 14.0. IR (KBr): 2968, 1628, 1516 cm<sup>-1</sup>. Anal. Calcd for C<sub>25</sub>H<sub>43</sub>NO<sub>2</sub>: C, 77.07; H, 11.12; N,  
12 3.60. Found: C, 77.13; H, 11.02; N, 3.60.

#### 23 24 25 b) Liberation of abietic acid from isopentylammonium abietate

26  
27 A suspension of isopentylammonium abietate (20 g, 0.05 mol) in diethyl ether (300 mL) was  
28 shaken vigorously with 5% hydrochloric acid (200 mL). Then the organic layer was separated  
29 and consecutively washed with water and brine. The ethereal layer was dried over sodium  
30 sulfate and evaporated to dryness. The residue was crystallized from ethanol-water affording  
31 14 g (89% yield) of pure abietic acid (**1**) as colorless crystals, mp 160–161 °C.  $[\alpha]_D^{22} -101.7$  (c  
32 0.6, EtOH). <sup>1</sup>H NMR (500 MHz, CDCl<sub>3</sub>): 5.77 (s, 1H), 5.38–5.35 (m, 1H), 2.22 (septet, *J* =  
33 6.8 Hz, 1H), 2.12–2.01 (m, 4H), 1.98–1.92 (m, 1H), 1.91–1.85 (m, 2H), 1.84–1.76 (m, 2H),  
34 1.71–1.65 (m, 1H), 1.62–1.55 (m, 2H), 1.26 (s, 3H), 1.26–1.09 (m, 2H), 1.01 (d, *J* = 6.8 Hz,  
35 3H), 1.00 (d, *J* = 6.8 Hz, 3H), 0.83 (s, 3H). <sup>13</sup>C NMR (125 MHz, CDCl<sub>3</sub>): δ 184.4, 145.3,  
36 135.6, 122.4, 120.5, 50.9, 46.3, 44.9, 38.3, 37.2, 34.9, 34.5, 27.4, 25.6, 22.5, 21.4, 20.9, 18.0,  
37 16.7, 14.0. IR (KBr): 2956, 1693, 1461 cm<sup>-1</sup>. HRMS (ESI) *m/z*: [M+Na]<sup>+</sup> Calcd for  
38 C<sub>20</sub>H<sub>30</sub>O<sub>2</sub>Na 325.2143; Found 325.2143.

#### 39 40 41 42 43 44 45 46 47 48 49 50 51 52 53 54 **Preparation of methyl abietate 10**

1  
2  
3 An ethereal solution of diazomethane was added dropwise to a stirred solution of abietic acid  
4 (**1**) (2 g, 6.7 mmol) in diethyl ether (50 mL) until evolution of nitrogen ceased and a slight  
5 yellow color persisted. The excess of diazomethane was destroyed by addition of a few drops  
6 of formic acid. Evaporation of ether afforded 2 g (97% yield) of methyl ester **10** as a colorless  
7 oil.  $[\alpha]_D^{22} -89.3$  (c 0.6, CHCl<sub>3</sub>). <sup>1</sup>H NMR (500 MHz, CDCl<sub>3</sub>): δ 5.77 (s, 1H), 5.37–5.34 (m,  
8 1H), 3.63 (s, 3H), 2.22 (septet,  $J = 6.8$  Hz, 1H), 2.11–2.01 (m, 4H), 1.97–1.92 (m, 1H), 1.90–  
9 1.85 (m, 1H), 1.84–1.68 (m, 3H), 1.64–1.53 (m, 3H), 1.25 (, 3H), 1.25–1.10 (m, 2H), 1.01 (d,  
10  $J = 6.8$  Hz, 3H), 1.00 (d,  $J = 6.8$  Hz, 3H), 0.82 (s, 3H). <sup>13</sup>C NMR (125 MHz, CDCl<sub>3</sub>): δ 179.0,  
11 145.3, 135.6, 122.4, 120.6, 51.8, 51.0, 46.6, 45.1, 38.3, 37.1, 34.9, 34.6, 27.5, 25.7, 22.5, 21.4,  
12 20.8, 18.1, 17.0, 14.0. IR (film): 2951, 2869, 1728 893 cm<sup>-1</sup>. HRMS (ESI)  $m/z$ : [M+Na]<sup>+</sup>  
13  
14  
15  
16  
17  
18  
19  
20  
21  
22  
23  
24 Calcd for C<sub>21</sub>H<sub>32</sub>O<sub>2</sub>Na 339.2300; Found 339.2304.  
25  
26

### 27 Preparation of diol **11**

28  
29 A mixture of methyl abietate (**10**) (2 g, 6.3 mmol), *tert*-butyl alcohol (30 mL), water (3 mL)  
30 osmium tetroxide (15 mg, 0.06 mmol) and *N*-methylmorpholine *N*-oxide (1g, 8.5 mmol) was  
31 stirred at 35 °C for one week. After this time an additional portion of osmium tetroxide (10  
32 mg, 0.04 mmol) and *N*-methylmorpholine *N*-oxide (1 g, 8.5 mmol) was added, and the  
33 reaction was continued for the next one week. Then an excess of oxidants was destroyed by  
34 addition of sodium sulfite (4 g, 32 mmol) to the reaction mixture. After one hour of vigorous  
35 agitation, the mixture was poured into water and extracted with methylene chloride. The  
36 organic layer was dried over anhydrous sodium sulfate and evaporated to dryness. The residue  
37 was chromatographed on silica gel (15% ethyl acetate in hexanes) yielding 1.5 g (66%) of  
38 diol **11** as a pale yellow oil.  $[\alpha]_D^{22} -18.3$  (c 0.5, CHCl<sub>3</sub>). <sup>1</sup>H NMR (500 MHz, CDCl<sub>3</sub>): δ 5.91–  
39 5.86 (m, 1H), 3.96 (br s, 1H), 3.64 (s, 3H), 2.17 (septet,  $J = 6.9$ Hz, 1H), 2.06–1.97 (m, 1H),  
40 1.93–1.84 (m, 2H), 1.82–1.51 (m, 10H), 1.46–1.28 (m, 2H), 1.27 (s, 3H), 1.17–1.08 (m, 1H),  
41 0.95 (d,  $J = 6.9$  Hz, 3H), 0.92 (d,  $J = 6.9$  Hz, 3H), 0.87 (s, 3H). <sup>13</sup>C NMR (125 MHz, CDCl<sub>3</sub>):  
42  
43  
44  
45  
46  
47  
48  
49  
50  
51  
52  
53  
54  
55  
56  
57  
58  
59  
60

1  
2  
3  $\delta$  179.1, 137.9, 120.0, 76.1, 73.2, 51.9, 51.2, 46.5, 44.6, 39.1, 37.0, 35.2, 33.0, 26.4, 25.0,  
4  
5 19.2, 18.0, 17.8, 17.4, 16.3, 15.5. IR (film): 3358, 2983, 1722  $\text{cm}^{-1}$ . HRMS (EI)  $m/z$ :  $[\text{M}]^+$   
6  
7 Calcd for  $\text{C}_{21}\text{H}_{34}\text{O}_4$  350.2457; Found 350.2451.  
8  
9

### 10 Preparation of hydroxyenone 2

11 A mixture of diol **11** (1.2 g, 3.4 mmol), diphenyl diselenide (1.6 g, 5.1 mmol), 5.5M *tert*-butyl  
12 hydroperoxide in decane (1.5 mL, 14.0 mmol) and carbon tetrachloride (60 mL) was refluxed  
13  
14 for 2 hrs. Then the excess of oxidant was decomposed by addition of isopropyl alcohol (2  
15  
16 mL), and the solvent was evaporated to dryness. The residue was chromatographed on silica  
17  
18 gel (5% ethyl acetate in hexanes) yielding 1.1 g (90%) of **2** as a pale yellow oil.  $[\alpha]_D^{22} +62.8$  (c  
19  
20 0.4,  $\text{CHCl}_3$ ).  $^1\text{H}$  NMR (500 MHz,  $\text{CDCl}_3$ ):  $\delta$  7.01–6.98 (m, 1H), 3.67 (s, 3H), 2.99 (br s, 1H),  
21  
22 2.32–2.26 (m, 1H), 2.20–1.81 (m, 7H), 1.79–1.64 (m, 3H), 1.63–1.58 (m, 2H), 1.38–1.27 (m,  
23  
24 1H), 1.25 (s, 3H), 1.19–1.11 (m, 1H), 0.91 (d,  $J = 6.7$  Hz, 3H), 0.81 (d,  $J = 6.8$  Hz, 3H), 0.76  
25  
26 (s, 3H).  $^{13}\text{C}$  NMR (125 MHz,  $\text{CDCl}_3$ ):  $\delta$  204.2, 187.4, 137.9, 135.4, 77.7, 52.0, 51.1, 46.2,  
27  
28 44.2, 37.7, 37.1, 35.6, 34.9, 31.6, 26.5, 19.0, 17.9, 16.64, 16.57, 16.2, 13.6. IR (film,  $\text{CH}_2\text{Cl}_2$ ):  
29  
30 3483, 2949, 1725, 1685, 1613  $\text{cm}^{-1}$ . HRMS (EI)  $m/z$ :  $[\text{M}]^+$  Calcd for  $\text{C}_{21}\text{H}_{32}\text{O}_4$  348.2301;  
31  
32 Found 348.2301.  
33  
34  
35  
36  
37  
38

### 39 Preparation of enones 3 and 4

40 A mixture of hydroxyenone **2** (720 mg, 2.1 mmol), zinc dust (1.3 g, 20 mmol), ammonium  
41  
42 chloride (140 mg, 2.6 mmol) and methanol (30 mL) was stirred at 50 °C for one week. After  
43  
44 this time an additional portion of zinc (0.7g, 10 mmol) and ammonium chloride (70 mg, 1,3  
45  
46 mmol) was added, and the reaction was continued for a week. Then all insoluble material was  
47  
48 filtered off and washed with methanol. The filtrate was poured into water and extracted with  
49  
50 ether. The organic layer was washed with brine, dried over sodium sulfate and evaporated to  
51  
52 dryness. The residue was chromatographed on silica gel (5% ethyl acetate in hexanes)  
53  
54 yielding 327 mg (48%) of enone **3** and 114 mg (17%) of enone **4**. **3**: colorless crystals, mp  
55  
56  
57  
58  
59  
60

1  
2  
3 75–76 °C.  $[\alpha]_D^{22} +30.5$  (c 0.5,  $\text{CHCl}_3$ ).  $^1\text{H}$  NMR (500 MHz,  $\text{C}_6\text{D}_6$ ):  $\delta$  7.00–6.96 (m, 1H), 3.32  
4 (s, 3H), 2.71 (septet of d,  $J = 6.9, 3.3$  Hz, 1H), 2.08 (dd,  $J = 9.8, 7.0$  Hz, 1H), 1.87–1.74 (m,  
5 5H), 1.65–1.59 (m, 1H), 1.59–1.48 (m, 3H), 1.43–1.30 (m, 2H), 1.19 (s, 3H), 1.14 (qd,  $J =$   
6 5H), 1.65–1.59 (m, 1H), 1.59–1.48 (m, 3H), 1.43–1.30 (m, 2H), 1.19 (s, 3H), 1.14 (qd,  $J =$   
7 13.0, 2.4 Hz, 1H), 0.94 (qd,  $J = 12.7, 2.5$  Hz, 1H), 0.91 (d,  $J = 6.8$  Hz, 3H), 0.88 (d,  $J = 7.1$   
8 Hz, 3H), 0.82 (td,  $J = 12.7, 4.7$  Hz, 1H), 0.61 (s, 3H).  $^{13}\text{C}$  NMR (125 MHz,  $\text{C}_6\text{D}_6$ ): 199.1,  
9 177.8, 137.4, 135.0, 54.8, 53.1, 51.5, 46.3, 44.3, 38.0, 37.3, 34.8, 27.5, 26.3, 22.7, 22.3, 20.5,  
10 18.32, 18.29, 17.0, 14.1. IR (film,  $\text{CH}_2\text{Cl}_2$ ): 2949, 1726, 1685, 1618  $\text{cm}^{-1}$ . HRMS (EI)  $m/z$ :  
11  $[\text{M}]^+$  Calcd for  $\text{C}_{21}\text{H}_{32}\text{O}_3$  332.2351; Found 332.2349. Anal. Calcd for  $\text{C}_{21}\text{H}_{32}\text{O}_3$ : C, 75.86; H,  
12 9.70. Found: C, 75.84; H, 9.77. **4**: colorless crystals, mp 84–85 °C.  $[\alpha]_D^{22} -86.1$  (c 0.7, EtOH).  
13  $^1\text{H}$  NMR (500 MHz,  $\text{C}_6\text{D}_6$ ):  $\delta$  6.82–6.80 (m, 1H), 3.32 (s, 3H), 2.10 (dd,  $J = 9.5, 7.3$  Hz, 1H),  
14 2.06–1.97 (m, 2H), 1.90–1.74 (m, 4H), 1.65 (dq,  $J = 13.9, 4.2$  Hz, 1H), 1.57–1.54 (m, 1H),  
15 1.51–1.46 (m, 1H), 1.19 (s, 3H), 1.15 (dd,  $J = 12.5, 4.4$  Hz, 1H), 0.97 (d,  $J = 6.3$  Hz, 3H),  
16 0.82 (d,  $J = 6.3$  Hz, 3H), 0.85–0.77 (m, 1H), 0.61 (s, 3H).  $^{13}\text{C}$  NMR (125 MHz,  $\text{C}_6\text{D}_6$ ):  $\delta$   
17 201.0, 177.9, 138.0, 133.7, 53.2, 51.7, 51.5, 46.4, 44.5, 38.1, 37.3, 34.9, 27.5, 26.1, 23.8, 21.1,  
18 19.4, 18.9, 18.3, 17.0, 14.0. IR (film,  $\text{CH}_2\text{Cl}_2$ ): 2950, 1726, 1685, 1621  $\text{cm}^{-1}$ . HRMS (ESI)  
19  $m/z$ :  $[\text{M}+\text{Na}]^+$  Calcd for  $\text{C}_{21}\text{H}_{32}\text{O}_3\text{Na}$  355.2249; Found 355.2249. Anal. Calcd for  $\text{C}_{21}\text{H}_{32}\text{O}_3$ :  
20 C, 75.86; H, 9.70. Found: C, 75.97; H, 9.61.

### Preparation of enone **12**

21  
22  
23  
24  
25  
26  
27  
28  
29  
30  
31  
32  
33  
34  
35  
36  
37  
38  
39  
40  
41 A mixture of methyl abietate (**10**) (3.4 g, 11.0 mmol), diethyl ether (60 mL), water (4 mL),  
42 potassium bicarbonate (10 g, 0.1 mol) and iodine (8.4 g, 33.1 mmol) was stirred at 30 °C for 4  
43 hrs. Then an excess of iodine was destroyed by addition of sodium sulfite (13 g, 0.10 mol),  
44 the reaction mixture was poured into water and extracted with diethyl ether. The organic layer  
45 was washed with brine, dried over sodium sulfate and evaporated to dryness. The residue was  
46 chromatographed on silica gel to yield 1.8 g (47%) of enone **12**. Colorless crystals, mp 86–88  
47 °C.  $[\alpha]_D^{22} -24.2$  (c 0.5,  $\text{CH}_2\text{Cl}_2$ );  $^1\text{H}$  NMR (500 MHz,  $\text{CDCl}_3$ ):  $\delta$  5.81 (s, 1H), 3.64 (s, 3H),  
48  
49  
50  
51  
52  
53  
54  
55  
56  
57  
58  
59  
60

1  
2  
3 2.88 (br d,  $J = 10$  Hz, 1H), 2.41 (t,  $J = 14.2$  Hz, 1H), 2.22 (septet,  $J = 6.8$  Hz, 1H), 2.15 (dd,  $J$   
4 = 14.2, 3.0 Hz, 1H), 2.08–1.84 (m, 5H), 1.80–1.71 (m, 1H), 1.70–1.59 (m, 3H), 1.37–1.28 (m,  
5 2H), 1.22 (s, 3H), 1.07 (s, 3H), 1.14–1.05 (m, 1H), 1.00 (d,  $J = 6.8$  Hz, 6H).  $^{13}\text{C}$  NMR (125  
6 MHz,  $\text{CDCl}_3$ ):  $\delta$  208.8, 177.8, 144.6, 115.2, 52.9, 52.1, 49.1, 48.8, 47.2, 40.9, 37.3, 36.8,  
7 36.0, 34.8, 26.6, 22.5, 21.6, 21.1, 17.8, 16.0, 13.6. IR (film,  $\text{CH}_2\text{Cl}_2$ ): 2952, 2869, 1727, 1713,  
8 1461  $\text{cm}^{-1}$ . HRMS (ESI)  $m/z$ :  $[\text{M}+\text{Na}]^+$  Calcd for  $\text{C}_{21}\text{H}_{32}\text{O}_3\text{Na}$  355.2249; Found 355.2253.  
9  
10  
11  
12  
13  
14  
15  
16  
17  
18  
19  
20  
21  
22  
23  
24  
25  
26  
27  
28  
29  
30  
31  
32  
33  
34  
35  
36  
37  
38  
39  
40  
41  
42  
43  
44  
45  
46  
47  
48  
49  
50  
51  
52  
53  
54  
55  
56  
57  
58  
59  
60

Anal. Calcd for  $\text{C}_{21}\text{H}_{32}\text{O}_3$ : C, 75.86; H, 9.70. Found: C, 75.67; H, 9.77.

### Preparation of hydroperoxides **6** and **7**

A solution of enone **12** (105 mg, 0.32 mmol) in THF (5 mL) and triethylamine (0.3 mL) was kept at room temperature for 24 hrs with access to air. Then solvents were evaporated to dryness. The residue was chromatographed on silica gel to yield **6** (86 mg, 74%) and **7** (14 mg, 12%). **6**: colorless crystals, mp 123–125 °C.  $[\alpha]_D^{22} +24.4$  (c 0.6, MeOH).  $^1\text{H}$  NMR (500 MHz,  $\text{CDCl}_3$ ):  $\delta$  7.31 (br s, 1H), 6.81–6.79 (m, 1H), 3.66 (s, 3H), 2.42–2.20 (m, 4H), 2.08–2.04 (m, 1H), 1.89–1.81 (m, 2H), 1.79–1.43 (m, 7H), 1.25 (s, 3H), 1.24–1.17 (m, 1H), 0.91 (d,  $J = 6.9$  Hz, 3H), 0.88 (s, 3H), 0.85 (d,  $J = 6.9$  Hz, 3H).  $^{13}\text{C}$  MNR (125 MHz,  $\text{CDCl}_3$ ):  $\delta$  198.9, 178.1, 141.3, 136.8, 83.3, 52.2, 51.5, 46.3, 44.4, 38.7, 38.0, 36.9, 35.5, 32.7, 25.8, 18.7, 17.8, 17.2, 16.4, 16.2, 14.4. IR (KBr): 3279, 2934, 1725, 1677, 1614  $\text{cm}^{-1}$ . HRMS (ESI)  $m/z$ :  $[\text{M} + \text{Na}]^+$  Calcd for  $\text{C}_{21}\text{H}_{32}\text{O}_5\text{Na}$  387.2147; Found 387.2139. Anal. Calcd for  $\text{C}_{21}\text{H}_{32}\text{O}_5$ : C, 69.20; H, 8.85. Found: C, 69.23; H, 8.78. **7**: colorless crystals, mp 114–116 °C;  $[\alpha]_D^{22} -73.7$  (c 0.3, MeOH);  $^1\text{H}$  NMR (600 MHz,  $\text{CDCl}_3$ ):  $\delta$  7.98 (br s, 1H), 6.84 (dd,  $J = 2.3, 1.6$  Hz, 1H), 3.66 (s, 3H), 2.39–2.33 (m, 2H), 2.28–2.21 (m, 2H), 1.97 (septet,  $J = 7.0$  Hz, 1H), 1.95–1.87 (m, 2H), 1.83 (qd,  $J = 13.3, 4.0$  Hz, 1H), 1.78–1.64 (m, 4H), 1.64–1.53 (m, 1H), 1.44–1.36 (m, 1H), 1.23 (s, 3H), 1.25–1.17 (m, 1H), 0.96 (d,  $J = 6.9$  Hz, 3H), 0.91 (d,  $J = 7.1$  Hz, 3H), 0.84 (s, 3H).  $^{13}\text{C}$  NMR (150 MHz,  $\text{CDCl}_3$ ):  $\delta$  199.4, 178.0, 140.6, 139.0, 84.8, 52.2, 50.5, 46.3, 44.5, 38.7, 37.5, 36.8, 35.6, 34.8, 25.8, 21.2, 17.9, 17.7, 16.8, 16.3, 14.3. IR (KBr): 3298,

1  
2  
3 2949, 1723, 1684, 1620  $\text{cm}^{-1}$ . HRMS (ESI)  $m/z$ :  $[\text{M}+\text{Na}]^+$  Calcd for  $\text{C}_{21}\text{H}_{32}\text{O}_5\text{Na}$  387.2147;  
4  
5 Found 387.2137. Anal. Calcd for  $\text{C}_{21}\text{H}_{32}\text{O}_5$ : C, 69.20; H, 8.85. Found: C, 69.05; H, 8.83.

### 6 7 **Isomerization of enone 12 to conjugated enone 5**

8  
9 Argon was bubbled through a refluxing toluene over 1 hr. Enone **12** (33 mg, 0.10 mmol) and  
10 sodium *tert*-butoxide (1 mg, 0.01 mmol) were placed in two separate flasks under argon. Then  
11 the deoxygenated toluene (2 mL) was transferred by cannula into the flask with **12**, and the  
12 resulted solution was transferred by cannula to the flask containing sodium *tert*-butoxide. The  
13 mixture was stirred under argon at room temperature over 24 hrs. and then quenched with  
14 deoxygenated 0.1% hydrochloric acid (4 mL). The mixture was poured into water and  
15 extracted with toluene. The organic layer was dried over sodium sulfate and evaporated to  
16 dryness. Conjugated enone **5** was separated from unchanged enone **12** by preparative TLC  
17 chromatography (two TLC plates 20x20 cm, 0.25 mm, 20% *tert*-butyl methyl ether in n-  
18 hexane). A spot visible in UV light, containing enone **5** was scratched out and washed with  
19 5% methanol in methylene chloride (3 mL). The solvent was blown out in a stream of argon.  
20  
21 12 mg of a dry residue was obtained.  $^1\text{H}$  NMR spectrum of the sample revealed that partial  
22 oxidation of the product **5** occurred and hydroperoxides **6** and **7** were formed.  $^1\text{H}$  NMR (500  
23 MHz,  $\text{CDCl}_3$ ), diagnostic signals only:  $\delta$  6.79-6.81 (m, 0.45H, assigned to vinyl proton of **6**),  
24 6.85 (bd,  $J = 2.26$  Hz, 0.06H, assigned to vinyl proton of **7**), 7.02 (0.49H, assigned to vinyl  
25 proton of **5**), 7.27 (bs, 0.45H, -OOH of **6**), 7.50 (bs, 0.06H, -OOH of **7**); HRMS (ESI) calcd  
26 for  $\text{C}_{21}\text{H}_{32}\text{O}_3\text{Na}$   $[\text{M}+\text{Na}]^+$  (assigned for **5**) 355.2249, found 355.2249; HRMS (ESI) calcd for  
27  $\text{C}_{21}\text{H}_{32}\text{O}_5\text{Na}$   $[\text{M}+\text{Na}]^+$  (assigned for **6** and **7**) 387.2147, found 387.2141.

### 28 29 30 31 32 33 34 35 36 37 38 39 40 41 42 43 44 45 46 47 48 **Preparation of enones 8, 9 and 13**

49  
50 A mixture of enone **12** (100 mg, 0.30 mmol), sodium *tert*-butoxide (1.5 mg, 0.016 mmol) and  
51 anhydrous toluene (3.0 mL) was stirred with access to air at room temperature for 24 hrs.  
52  
53 Then the mixture was poured into water and extracted with toluene. The organic layer was  
54  
55  
56  
57  
58  
59  
60

dried over sodium sulfate and evaporated to dryness. The residue was chromatographed on silica gel (10% ethyl acetate in hexanes) to yield **13** (36 mg, 34%), **8** (27 mg, 26%) and **9** (12 mg, 11%) in elution order. **13**: Colorless crystals, mp 115–117 °C.  $[\alpha]_D^{22}$  –42.0 (c 0.5, EtOH).  $^1\text{H}$  NMR (500 MHz,  $\text{CDCl}_3$ ):  $\delta$  5.25 (s, 1H), 3.88 (s, 1H, OH exchangeable with  $\text{D}_2\text{O}$ ), 3.67 (s, 3H), 2.52 (t,  $J = 14.1$  Hz, 1H), 2.26–2.16 (m, 3H), 2.14–2.04 (m, 3H), 1.94–1.92 (m, 2H), 1.77–1.70 (m, 2H), 1.67–1.56 (m, 4H), 1.22 (s, 3H), 1.11 (s, 3H), 1.01 (d,  $J = 6.9$  Hz, 6H).  $^{13}\text{C}$  NMR (125 MHz,  $\text{CDCl}_3$ ):  $\delta$  212.9, 177.8, 151.3, 118.9, 74.9, 55.1, 52.2, 47.6, 47.1, 39.8, 38.38, 38.35, 36.6, 35.2, 24.1, 21.2, 20.9, 17.5, 17.3, 16.7, 15.1. IR (film,  $\text{CH}_2\text{Cl}_2$ ): 3477, 2952, 1725, 1619  $\text{cm}^{-1}$ . HRMS (ESI)  $m/z$ :  $[\text{M}+\text{Na}]^+$  Calcd for  $\text{C}_{21}\text{H}_{32}\text{O}_4\text{Na}$  371.2198; Found 371.2196. Anal. Calcd for  $\text{C}_{21}\text{H}_{32}\text{O}_4$ : C, 72.38; H, 9.25. Found: C, 72.24; H, 9.13. **8**: Colorless oil.  $[\alpha]_D^{22}$  +8.7 (c 0.6, EtOH).  $^1\text{H}$  NMR (500 MHz,  $\text{CDCl}_3$ ):  $\delta$  6.74 (br s, 1H), 3.66 (s, 3H), 2.40–2.24 (m, 3H), 2.10–2.05 (m, 1H), 1.86 (br d,  $J = 13.0$  Hz, 1H), 1.80–1.68 (m, 4H), 1.66–1.60 (m, 2H), 1.60–1.53 (m, 2H), 1.50–1.45 (m, 2H), 1.25 (s, 3H), 1.25–1.18 (m, 1H), 0.96 (d,  $J = 6.8$  Hz, 3H), 0.88 (s, 3H), 0.86 (d,  $J = 6.9$  Hz, 3H).  $^{13}\text{C}$  NMR (125 MHz,  $\text{CDCl}_3$ ):  $\delta$  199.3, 178.1, 140.1, 138.4, 71.8, 52.1, 51.7, 46.3, 44.4, 38.6, 37.9, 37.8, 36.9, 35.5, 29.5, 18.3, 17.8, 17.3, 16.4, 16.1, 14.4. IR (film,  $\text{CH}_2\text{Cl}_2$ ): 3455, 2951, 1726, 1685, 1613  $\text{cm}^{-1}$ . HRMS (ESI)  $m/z$ :  $[\text{M}+\text{Na}]^+$  Calcd for  $\text{C}_{21}\text{H}_{32}\text{O}_4\text{Na}$  371.2198; Found 371.2195. Anal. Calcd for  $\text{C}_{21}\text{H}_{32}\text{O}_4$ : C, 72.38; H, 9.25. Found: C, 72.24; H, 9.42. **9**: Colorless crystals, mp 130–131 °C.  $[\alpha]_D^{22}$  –72.0 (c 0.3, EtOH).  $^1\text{H}$  NMR (500 MHz,  $\text{CDCl}_3$ ):  $\delta$  6.75 (br s, 1H), 3.66 (s, 3H), 2.39–2.31 (m, 2H), 2.28–2.20 (m, 2H), 2.17–2.12 (m, 1H), 1.82–1.55 (m, 7H), 1.48–1.36 (m, 3H), 1.27–1.17 (m, 1H), 1.24 (s, 3H), 0.98 (d,  $J = 6.8$  Hz, 3H), 0.94 (d,  $J = 6.8$  Hz, 3H), 0.86 (s, 3H).  $^{13}\text{C}$  NMR (125 MHz,  $\text{CDCl}_3$ ):  $\delta$  199.5, 178.0, 141.3, 136.8, 72.5, 52.2, 50.7, 46.4, 45.1, 39.0, 37.4, 36.8, 36.2, 35.9, 32.8, 20.5, 17.8, 17.0, 16.7, 16.2, 14.1. IR (film,  $\text{CH}_2\text{Cl}_2$ ): 3476, 2948, 1725, 1686, 1616  $\text{cm}^{-1}$ . HRMS (ESI)  $m/z$ :  $[\text{M}+\text{Na}]^+$  Calcd for  $\text{C}_{21}\text{H}_{32}\text{O}_4\text{Na}$  371.2198; Found 371.2201. Anal. Calcd for  $\text{C}_{21}\text{H}_{32}\text{O}_4$ : C, 72.38; H, 9.25. Found: C, 72.43; H, 9.32.

### Reduction of hydroperoxide **6**

A mixture of hydroperoxide **6** (5.5 mg, 0.015 mmol), triphenylphosphine (4.2 mg, 0.016 mmol) and dichloromethane (0.7 mL) was stirred at room temperature for 1 hr and then transferred on TLC plate and chromatographed (30% ethyl acetate in hexane). A colorless oil (4.8 mg, 87%) identical ( $^1\text{H}$  NMR,  $^{13}\text{C}$  NMR) with alcohol **8** previously described was afforded.

### Reduction of hydroperoxide **7**

A mixture of hydroperoxide **7** (9,5 mg, 0.026 mmol), triphenylphosphine (7.2 mg, 0.027 mmol) and dichloromethane (1.7 mL) was stirred at room temperature for 1 hr and then transferred on TLC plate and chromatographed (30% ethyl acetate in hexane). A colorless solid (6.8 mg, 71%) identical ( $^1\text{H}$  NMR,  $^{13}\text{C}$  NMR) with alcohol **9** previously described was afforded.

## ASSOCIATED CONTENT

### Supporting Information

$^1\text{H}$  and  $^{13}\text{C}$  NMR spectra of all synthesized compounds;

$^{13}\text{C}$ - $^{13}\text{C}$  2D INADEQUATE spectra of compounds **3** and **4**;

IR spectroscopy dilution experiments of compound **2** in  $\text{CCl}_4$ ;

Cartesian coordinates and simulated ECD spectra for individual conformers of enones **2-13**;

Crystallographic data for **3**, **6**, **9**, **12** and **13** (CIF).

## ACKNOWLEDGMENTS

This work was supported by the National Science Centre, grant No. UMO-2011/01/B/ST5/06413. All calculations were performed at the Interdisciplinary Centre for Mathematical and Computational Modeling, University of Warsaw (ICM UW), Poland, Grants No. G 36-12 and No. G 34-15.

## References

1. Nguyen, L. A.; Hua He, H.; Pham-Huy, C. *Int. J. Biomed. Sci.* **2006**, *2*, 85.

2. (a) Pescitelli, G.; Di Bari, I.; Berova, N. *Chem. Soc. Rev.* **2011**, *40*, 4603. (b) Mazzanti, A.; Casarini, D. *WIREs* **2012**, *2*, 613.
3. (a) Polavarapu, P. L., *Chirality* **2016**, *28*, 445. (b) Nugroho, A. E.; Morita, H. *J. Nat. Med.* **2014**, *68*, 1. (c) Pescitelli, G.; Bruhn, T. *Chirality* **2016**, *28*, 466. (d) Masnyk, M.; Butkiewicz, A.; Górecki, M.; Luboradzki, R.; Bannwarth, C.; Grimme, S.; Frelek, J. *J. Org. Chem.* **2016**, *81*, 4588. (e) Polavarapu, P. L., *Chiroptical Spectroscopy: Fundamentals and Applications*. CRC Press: **2016**. (f) Zhang, J.; Gholami, H.; Ding, X.; Chun, M.; Vasileiou, C.; Nehira, T.; Borhan, B., *Org. Lett.* **2017**, *19*, 1362. (g) Tanaka, H.; Inoue, Y.; Nakano, T.; Mori, T. *Photochem. Photobiol. Sci.* **2017**, *16*, 606.
4. (a) Gawroński, J. K. *Tetrahedron* **1982**, *38*, 3. (b) Kirk, D. N., *Tetrahedron* **1986**, *42*, 777. (c) Patai, S.; Rappoport, Z. *The Chemistry of Enones*. Wiley-VCH: Chichester, New York, Brisbane, Toronto, Singapore, **1989**; Vol. 1, p 55-105. (d) Lightner, D. A.; Gurst, J. E., *Organic Conformational Analysis and Stereochemistry from Circular Dichroism Spectroscopy*. Wiley-VCH: New York, **2000**. (e) N. Berova; P. Polavarapu; Nakanishi, K.; Woody, R. W., *Comprehensive Chiroptical Spectroscopy*. Wiley-VCH: New York, Chichester, Weinheim, Brisbane, Singapore, Toronto, **2012**; p 39-55.
5. (a) Cordell, G. A., *The Alkaloids: Chemistry and Pharmacology*. Elsevier Inc.: **1997**; p 1-405; (b) Overton, K. H., *Terpenoids and Steroids*,. The Chemical Society: London, **1974**; Vol. 4, p 1-608. (c) Lednicer, D., *Steroid Chemistry at a Glance*. Wiley: Chichester, **2010**; p 1-152. (d) Tolstikova, T. G.; Sorokina, I. V.; Tolstikov, G. A.; Tolstikov, A. G.; Flekhter, O. B., *Russian J. Bioorg. Chem.* **2006**, *32*, 37.
6. (a) Frelek, J.; Szczepek, W. J.; Neubrech, S.; Schultheis, B.; Brechtel, J.; Kuball, H.-G., *Chem. –Eur. J.* **2002**, *8*, 1899. (b) Frelek, J.; Butkiewicz, A.; Gorecki, M.; Wojcieszczyk, R. K.; Luboradzki, R.; Kwit, M.; Rode, M. F.; Szczepek, W. J., *RSC Advances* **2014**, *4*, 43977. (c) Stončius, S.; Neniškis, A.; Loganathan, N.; Wendt, O. F. *Chirality* **2015**, *27*, 728. (d) Pescitelli, G.; Di Bari, L. *Chirality* **2017**, *29*, 476.
7. (a) P. Kraft; J. A. Bajgrowicz; C. Denis; Fráter, G., *Angew. Chem. Int. Ed.* **2000**, *39*, 2980. (b) Castro, J. M.; Salido, S.; Altarejos, J.; Nogueras, M.; Sánchez, A., *Tetrahedron* **2002**, *58*, 5941. (c) Fráter, G.; Bajgrowicz, J. A.; Kraft, P. *Tetrahedron* **1998**, *54*, 7633. (d) Barrero, A. F.; Alvarez-Manzaneda, E. J.; Altarejos, J.; Salido, S.; Ramos, J. M. *Tetrahedron* **1993**, *49*, 10405. (e) Recio, M. C.; Giner, R. M.; Manez, S.; Rios, J. L., *Planta Med.* **1995**, *61*, 182. (f) San Feliciano, A.; Gordaliza, M.; Salinero, M. A.; Miguel del Corral, J. M., *Planta Med.* **1993**, *59*, 485.
8. (a) Ebrahimi, S. N. *Phytochemical Profiling of Iranian Plants, and ECD Calculation as Tool for Establishing the Absolute Configuration of New Natural Products*. PhD Thesis, Universität Basel, Basel, **2013**; (b) Andrade, R.; Ayer, W. A.; Trifonov, L. S., *Can. J. Chem.* **1996** *74*, 374. (c) Ebrahimi, S. N.; Zimmermann, S.; Zaugg, J.; Smiesko, M.; Brun, R.; Hamburger, M. *Planta Med.* **2013**, *79*, 150.
9. (a) Rafferty, R. J.; Hicklin, R. W.; Maloof, K. A.; Hergenrother, P. J. *Angew. Chem. Int. Ed.* **2014**, *53*, 220. (b) Alvarez-Manzaneda, E.; Chahboun, R.; Bentaleb, F.; Alvarez, E.; Escobar, M. A.; Sad-Diki, S.; Cano, M. J.; Messouri, I. *Tetrahedron* **2007**, *63*, 11204.
10. (a) Harris, G. C.; Sanderson, T. F. *Org. Synth.* **1952**, *32*, 1. (b) Roh, S.; Park, M.; Kim, Y. *J. Health Sci.* **2010**, *56*, 451. (c) González, M. A.; Correa-Royero, J.; Agudelo, L.; Mesa, A.; Betancur-Galvis, L. *Eur. J. Med. Chem.* **2009**, *44*, 2468. (d) He, Y.; Zhang, Y.; Lu, J.; Lin, R. *J. Pharm. Biomed. Anal.* **2012**, *66*, 345.
11. (a) Presser, A.; Haslinger, E.; Weis, R.; Hüfner, A. *Monatsh. Chem.* **1998**, *129*, 921. (b) Dos Santos, C.; Zukerman-Schpector, J.; Imamura, P. M., *J. Braz. Chem. Soc.* **2003**, *14*, 998.
12. Jawiczuk, M.; Górecki, M.; Masnyk, M.; Frelek, J. *Trends Anal. Chem.* **2015**, *73*, 119.

- 1  
2  
3 13. (a) Michalak, M.; Stodulski, M.; Stecko, S.; Woźnica, M.; Staszewska-Krajewska, O.;  
4 Kalicki, P.; Furman, B.; Frelek, J.; Chmielewski, M. *Tetrahedron* **2012**, *68*, 10806. (b)  
5 Roszkowski, P.; Błachut, D.; Maurin, J. K.; Woźnica, M.; Frelek, J.; Pluciński, F.; Czarnocki,  
6 *Z. Eur. J. Org. Chem.* **2013**, *35*, 7867.
- 7 14. Cilko, Y. A.; Raldugin, V. A.; Mamatyuk, V. I.; Shmidt, E. N.; Pentegova, V. A. *Izv.*  
8 *Sibir. Otd. Akad. Nauk Khim.* **1983**, *2*, 124.
- 9 15. Amato, M. E.; Ballistreri, F. P.; Pappalardo, A.; Tomaselli, G. A.; Toscano, R. M.;  
10 Trusso Sfrazzetto, G. *Molecules* **2013**, *18*, 13754.
- 11 16. García-Cabeza, A. L.; Marín-Barríos, R.; Azarken, R.; Moreno-Dorado, F. J.; Ortega,  
12 M. J.; Vidal, H.; Gatica, J. M.; Massanet, G. M.; Guerra, F. M. *Eur. J. Org. Chem.* **2013**, *36*,  
13 8307.
- 14 17. Kwit, M.; Skowronek, P.; Gawronski, J.; Frelek, J.; Woźnica, M.; Butkiewicz, A. *in:*  
15 *Comprehensive Chiroptical Spectroscopy; Some inherently chiral chromophores – empirical*  
16 *rules and quantum chemical calculations*. Eds.: Berova, N.; Polavarapu, P. L.; Nakanishi, K.;  
17 Woody, R. W., John Wiley and Sons, Inc: Hoboken, New Jersey, **2012**; Vol. 2, p 39-72.
- 18 18. *Conflex 7* Conflex Corporation, AIOS Meguro 6F, 2-15-19, Kami-Osaki Shinagawa-  
19 ku, 141-0021, Japan: Tokyo **2012**.
- 20 19. (a) Debie, E.; Bultinck, P.; Nafie, L. A. *CompareVOA*, BioTools Inc.: 17546 Bee Line  
21 Highway; Jupiter; FL 33458; USA, **2010**; (b) Debie, E.; De Gussem, E.; Dukor, R. K.;  
22 Herrebut, W.; Nafie, L. A.; Bultinck, P., *Chem. Phys. Chem.* **2011**, *12*, 1542.
- 23 20. Halgren, T. A. *J. Comp. Chem.* **1999**, *20*, 720.
- 24 21. Halgren, T. A. *J. Comput. Chem.* **1996**, *17*, 490.
- 25 22. (a) Becke, A. D., *J. Chem. Phys.* **1993**, *98*, 1372. (b) Yanai, T.; Tew, D. P.; Handy, N.  
26 *C. Chem. Phys. Lett.* **2004**, *393*, 51.
- 27 23. Becke, A. D. *J. Chem. Phys.* **1993**, *98*, 5648.
- 28 24. (a) Schaefer, A.; Horn, H.; Ahlrichs, R. *J. Chem. Phys.* **1992**, *97*, 2571. (b) Schaefer,  
29 A.; Huber, C.; Ahlrichs, R. *J. Chem. Phys.* **1994**, *100*, 5829.
- 30 25. (a) Dunning, T. H. *J. Chem. Phys.* **1989**, *90*, 1007. (b) Woon, D. E.; Dunning, T. H., *J.*  
31 *Chem. Phys.* **1995**, *103*, 4572.
- 32 26. Halgren, T. A., *J. Am. Chem. Soc.* 1992, *114*, 7827-7843.
- 33 27. Spartan'14 Wavefunction, Inc., 18401 Von Karman Avenue, Suite 370, Irvine, CA  
34 92612 USA.
- 35 28. Amovilli, C.; Barone, V.; Cammi, R.; Cancès, E.; Cossi, M.; Mennucci, B.; Pomelli,  
36 C. S.; Tomasi, J. Recent Advances in the Description of Solvent Effects with the Polarizable  
37 Continuum Model. In *Advances in Quantum Chemistry*, Per-Olov, L., Ed. Academic Press:  
38 **1998**; Vol. 32, pp 227-261.
- 39 29. Pescitelli, G. *Chirality* **2012**, *24*, 718.
- 40 30. Bruhn, T.; Schaumlöffel, A.; Hemberger, Y.; Bringmann, G. *Chirality* **2013**, *25*, 243.
- 41 31. Debie, E.; De Gussem, E.; Dukor, R. K.; Herrebut, W.; Nafie, L. A.; Bultinck, P.  
42 *Chem. Phys. Chem.* **2011**, *12*, 1542.
- 43 32. Wellman, K.; Djerassi, C. *J. Am. Chem. Soc.* **1963**, *85*, 3515.
- 44 33. Christiansen, O.; Hättig, C.; Jørgensen, P. *Spectrochim. Acta Mol. Biomol. Spectrosc.*  
45 **1999**, *55*, 509.
- 46 34. Agilent *CrysAlis PRO*. Agilent Technologies: Yarnton, England, **2011**.
- 47 35. Sheldrick, G. M., *Acta Cryst.* **2008**, *64*, 112.
- 48 36. M. J. Frisch; G. W. Trucks; H. B. Schlegel; G. E. Scuseria; M. A. Robb; J. R.  
49 Cheeseman; G. Scalmani; V. Barone; B. Mennucci; G. A. Petersson; H. Nakatsuji; M.  
50 Caricato; X. Li; H. P. Hratchian; A. F. Izmaylov; J. Bloino; G. Zheng; J. L. Sonnenberg; M.  
51 Hada; M. Ehara; K. Toyota; R. Fukuda; J. Hasegawa; M. Ishida; T. Nakajima; Y. Honda; O.  
52 Kitao; H. Nakai; T. Vreven; J. A. Montgomery, J.; J. E. Peralta; F. Ogliaro; M. Bearpark; J. J.

1  
2  
3 Heyd; E. Brothers; K. N. Kudin; V. N. Staroverov; R. Kobayashi; J. Normand; K.  
4 Raghavachari; A. Rendell; J. C. Burant; S. S. Iyengar; J. Tomasi; M. Cossi; N. Rega; J. M.  
5 Millam; M. Klene; J. E. Knox; J. B. Cross; V. Bakken; C. Adamo; J. Jaramillo; R. Gomperts;  
6 R. E. Stratmann; O. Yazyev, A.; J. Austin; R. Cammi; C. Pomelli; J. W. Ochterski; R. L.  
7 Martin; K. Morokuma; V. G. Zakrzewski; G. A. Voth, P. S.; J. J. Dannenberg; S. Dapprich;  
8 A. D. Daniels; Ö. Farkas; J. B. Foresman; J. V. Ortiz; J. Cioslowski; Fox, D. J. *Rev. E. 01*  
9 *Gaussian 09*, Gaussian, Inc.: Wallingford CT, **2009**.  
10 37. Junior, F. M. S.; Covington, C. L.; de Amorim, M. B.; Velozo, L. S. M.; Kaplan, M.  
11 A. C.; Polavarapu, P. L. *J. Nat. Prod.* **2014**, *77*, 1881.  
12  
13  
14  
15  
16  
17  
18  
19  
20  
21  
22  
23  
24  
25  
26  
27  
28  
29  
30  
31  
32  
33  
34  
35  
36  
37  
38  
39  
40  
41  
42  
43  
44  
45  
46  
47  
48  
49  
50  
51  
52  
53  
54  
55  
56  
57  
58  
59  
60